

This discussion paper is/has been under review for the journal Hydrology and Earth System Sciences (HESS). Please refer to the corresponding final paper in HESS if available.

# Geochemical inverse modeling of chemical and isotopic data from groundwaters in Sahara (Ouargla basin, Algeria)

R. Slimani<sup>1</sup>, A. Guendouz<sup>2</sup>, F. Trolard<sup>3</sup>, A. S. Moulla<sup>4</sup>, B. Hamdi-Aïssa<sup>1</sup>, and G. Bourrié<sup>3</sup>

<sup>1</sup>Univ. Ouargla, Fac. des sciences de la nature et de la vie, Lab. Biochimie des milieux désertiques, Ouargla 30000, Algeria

<sup>2</sup>Blida University, Science and Engineering Faculty, P.O. Box 270 Soumaa, Blida, Algeria

<sup>3</sup>INRA, UMR1114 Emmah, Avignon, France

<sup>4</sup>Algiers Nuclear Research Centre, P.O. Box 399 Alger-RP, Algiers 16000, Algeria

Received: 8 September 2015 – Accepted: 4 October 2015 – Published: 1 February 2015

Correspondence to: R. Slimani (slm\_rabia@yahoo.fr)

Published by Copernicus Publications on behalf of the European Geosciences Union.

Chemical and  
isotopic data from  
groundwaters in  
Sahara

R. Slimani et al.

Title Page

Abstract

Introduction

Conclusions

References

Tables

Figures

◀

▶

◀

▶

Back

Close

Full Screen / Esc

Printer-friendly Version

Interactive Discussion



## Abstract

New samples were collected in the three major Saharan aquifers namely, the “Continental Intercalaire” (CI), the “Complexe Terminal” (CT) and the Phreatic aquifer (Phr) and completed with unpublished more ancient chemical and isotopic data. Instead of classical Debye-Hückel extended law, Specific Interaction Theory (SIT) model, recently incorporated in Phreeqc 3.0 was used. Inverse modeling of hydro chemical data constrained by isotopic data was used here to quantitatively assess the influence of geochemical processes: at depth, the dissolution of salts from the geological formations during upward leakage without evaporation explains the tran sitions from CI to CT and to a first pole of Phr (pole I); near the surface, the dissolution of salts from sebkhas by rainwater explains another pole of Phr (pole II). In every case, secondary precipitation of calcite occurs during dissolution. All Phr waters result from the mixing of these two poles together with calcite precipitation and ion exchange processes. These processes are quantitatively assessed by Phreeqc model. Globally, gypsum dissolution and calcite precipitation were found to act as a carbon sink.

## 1 Introduction

A scientific study published in 2008 showed that 85 % of the world population lives in the driest half of the Earth. More than 1 billion people residing in arid and semi-arid areas of the world have only access to little or no renewable water resources (OECD, 2008). In many arid regions such as Sahara, groundwater is the only source of water supply for domestic, agricultural or industrial purposes, causing most of the time overuse and/or degradation of water quality.

The groundwater resources of Ouargla basin (Lower-Sahara, Algerian; Fig. 1) are contained in three main reservoirs (UNESCO, 1972; Eckstein and Eckstein, 2003; OSS, 2003, 2008):

<a href="#">Title Page</a>	
<a href="#">Abstract</a>	<a href="#">Introduction</a>
<a href="#">Conclusions</a>	<a href="#">References</a>
<a href="#">Tables</a>	<a href="#">Figures</a>
<a href="#">◀</a>	<a href="#">▶</a>
<a href="#">◀</a>	<a href="#">▶</a>
<a href="#">Back</a>	<a href="#">Close</a>
<a href="#">Full Screen / Esc</a>	
<a href="#">Printer-friendly Version</a>	
<a href="#">Interactive Discussion</a>	

- at the top, the phreatic aquifer (Phr), located in sandy gypsum permeable formations of Quaternary, is almost unexploited (only north of Ouargla) due to its salinity ( $50 \text{ g L}^{-1}$ );
- 5 – in the middle, the “Complexe Terminal” (CT) aquifer, (Cornet and Gouscov, 1952; UNESCO, 1972) which is the most exploited, and includes several aquifers in different geological formations. It circulates in one or two lithostratigraphic formations of the Eocene and Senonian carbonates or Mio-pliocene sands;
- 10 – at the bottom, the “Continental Intercalaire” (CI) aquifer, where water is contained in the lower Cretaceous continental formations (Barremian and Albian), mainly composed of sandstones, sands and clays. It is only partially exploited because of its significant depth.

After use, waters are discharged in a closed system (endorheic basin) and constitute a potential hazard to the environment, to public health and may jeopardize the sustainability of agriculture (rising of the phreatic aquifer watertable, extension of soil 15 salinization and so on; Hamdi-Aïssa et al., 2004; Slimani, 2006). Several previous studies (Guendouz, 1985; Fontes et al., 1986; Guendouz and Moulla, 1996; Edmunds et al., 2003; Guendouz et al., 2003; Hamdi-Aïssa et al., 2004; Foster et al., 2006; OSS, 2008; Al-Gamal, 2011) tried, starting from chemical and isotopic information ( $^2\text{H}$ ,  $^{18}\text{O}$ ,  $^{234}\text{U}$ ,  $^{238}\text{U}$ ,  $^{36}\text{Cl}$ ) to best characterize the relationships between aquifers. They were more 20 specifically tackling the issue of the Continental Intercalaire recharge. These investigations dealt particularly with water chemical facies, mapped isocontents of various parameters, and reported typical geochemical ratios ( $[\text{SO}_4^{2-}] / [\text{Cl}^-]$ ,  $[\text{Mg}^{2+}] / [\text{Ca}^{2+}]$ ) as well as other correlations. Minerals/solutions equilibria were checked by computing saturation indices with respect to calcite, gypsum, anhydrite and halite, but processes 25 were only qualitatively assessed.

In the present study, new data were collected in order to characterize the hydrochemical and the isotopic composition of the major aquifers in Ouargla' region. They also aimed at identifying the origin of the mineralization and water-rock interactions that

## Chemical and isotopic data from groundwaters in Sahara

R. Slimani et al.

[Title Page](#)

[Abstract](#)

[Introduction](#)

[Conclusions](#)

[References](#)

[Tables](#)

[Figures](#)

◀

▶

◀

▶

[Back](#)

[Close](#)

[Full Screen / Esc](#)

[Printer-friendly Version](#)

[Interactive Discussion](#)



occur along the flow. New possibilities offered by progress in geochemical simulations were used. More specifically, Specific Interaction Theory (SIT) recently incorporated in Phreeqc 3.0 (Parkhurst and Appelo, 2013) seems now to bridge the gap between the “extended” Debye-Hückel law that is valid only for dilute solutions and Pitzer’s model, which is mainly used for brines, and which appears now as over parameterized (Grenthe and Plyasunov, 1997). Inverse modeling with Phreeqc 3.0 was used to quantitatively assess the influence of the processes that explain the acquisition of solutes for the different aquifers: dissolution, precipitation, mixing and ion exchange. This results in constraints on mass balances as well as on the exchange of matter between aquifers.

## 10 2 Methodology

## **2.1 Presentation of the study area**

The study area is located in the northeastern desert of Algeria “Lower-Sahara” (Le Houérou, 2009) near the city of Ouargla (Fig. 1), 31°54' to 32°1' N and 5°15' to 5°27' E, with a mean elevation of 134 (m.a.s.l.). It is located in the quaternary fossil valley of Oued Mya basin. Present climate belongs to the arid Mediterranean-type (Dubreif, 1963; Le Houérou, 2009; ONM, 1975/2013). This climate is characterized by a mean annual temperature of 22.5 °C, a yearly rainfall of 43.6 mm yr<sup>-1</sup> and a very high evaporation rate of 2138 mm yr<sup>-1</sup>.

Geologically, Ouargla's region and the entire Lower Sahara consist of sedimentary formations (Fig. 2). The basin is carved into Mio-pliocene (MP) deposits, which alternate with red sands, clays and sometimes marls; gypsum is not abundant and dated from Pontian (MP; Cornet and Gouscov, 1952; Dubief, 1953; Ould Baba Sy and Besbes, 2006). The continental Pliocene consists of a local limestone crust with pudding-stone or lacustrine limestone (Fig. 2), shaped by æolian erosion into flat areas (regs). The Quaternary formations are lithologically composed of alternating layers of permeable sand and relatively impermeable marl (Aumassip et al., 1972; Chellat et al., 2014).

# Chemical and isotopic data from groundwaters in Sahara

R. Slimani et al.

Title Page

## Abstract

Introduction

## Conclusions

## References

Tables

## Figures



Bad

Close

Full Screen / Esc

[Printer-friendly Version](#)

## Interactive Discussion



The exploitation of Mio-pliocene aquifer is ancient and at the origin of the creation of the oasis (Lelièvre, 1969; Moulias, 1927). The piezometric level was higher (145 m a.s.l.) but overexploitation at the end of the XIXth century led to a catastrophic decrease of the resource, with presently more than 900 boreholes (ANRH, 2011).

5 The exploitation of Senonian aquifer dates back to 1953 at a depth 140 to 200 m depth, with a small initial rate ca.  $540 \text{ L mn}^{-1}$ ; two boreholes have been exploited since 1965 and 1969, with a total flowrate ca.  $2500 \text{ L mn}^{-1}$ , for drinking water and irrigation.

The exploitation of Albian aquifer dates back to 1956, with a piezometric level 405 m and a pressure  $22 \text{ kg cm}^{-2}$ . Presently, two boreholes are exploited:

- 10 – El Hedeby I, 1335 m depth, with a flowrate  $141 \text{ L s}^{-1}$ ;  
– El Hedeby II, 1400 m depth, with a flowrate  $68 \text{ L s}^{-1}$ .

## 2.2 Sampling and analytical methods

The sampling scheme complies with the flow directions of the two formations (Phr and CT aquifers); for the Cl aquifer only five points are available, so it is impossible 15 to choose a transect (Fig. 3). Groundwater samples ( $n = 107$ ) were collected during a field campaign in 2013, along the main flow line of Oued Mya, 67 piezometers tap the phreatic aquifer, 32 wells tap the CT aquifer and 8 boreholes tap the Cl aquifer (Fig. 3). Analyses of  $\text{Na}^+$ ,  $\text{K}^+$ ,  $\text{Ca}^{2+}$ ,  $\text{Mg}^{2+}$ ,  $\text{Cl}^-$ ,  $\text{SO}_4^{2-}$  and  $\text{HCO}_3^-$  were performed by ion chromatography at Algiers Nuclear Research Center (CRNA). Previous and yet 20 unpublished data (Guendouz and Moulla, 1996) sampled in 1996 are used here too: 59 samples for Phr aquifer, 15 samples for CT aquifer and 3 samples for the Cl aquifer for chemical analyses, data  $^{18}\text{O}$  and  $^3\text{H}$  (Guendouz and Moulla, 1996).

## 2.3 Geochemical method

Phreeqc (Parkhurst and Appelo, 2013) was used to check minerals/solution equilibria 25 using the specific interaction theory (SIT), i.e. the extension of Debye-Hückel law by

Scatchard and Guggenheim incorporated recently in Phreeqc 3.0. Inverse modeling was used to calculate the number of minerals and gases' moles that must respectively dissolve or precipitate/degas to account for the difference in composition between initial and final water end members (Plummer and Back, 1980; Kenoyer and Bowser, 1992; Deutsch, 1997; Plummer and Sprinkle, 2001; Guler and Thyne, 2004; Parkhurst and Appelo, 2013). This mass balance technique has been used to quantify reactions controlling water chemistry along flow paths (Thomas et al., 1989). It is also used to quantify the mixing proportions of end-member components in a flow system (Kuells et al., 2000; Belkhiri et al., 2010, 2012).

### 10 3 Results and discussion

Tables 1 to 5 illustrate the results of the chemical and the isotopic analyses. Samples are ordered according to an increasing salt content that was estimated from their specific electric conductivity (EC). In both phreatic and CT aquifers, temperature is close to 25 °C, while for Cl aquifer, temperature is close to 50 °C. The results presented in those tables are raw analytical data that were corrected for defects of charge balance before computing activities with Phreeqc. As analytical errors could not be ascribed to a specific analyte, the correction was made proportionally. The corrections do not affect the anions to anions mole ratios such as for  $[\text{HCO}_3^-]/([\text{Cl}^-]+2[\text{SO}_4^{2-}])$  or  $[\text{SO}_4^{2-}]/[\text{Cl}^-]$ , whereas they affect the cation to anion ratio such as for  $[\text{Na}^+]/[\text{Cl}^-]$ .

#### 20 3.1 Characterization of chemical facies of the groundwater

Piper diagrams drawn for the studied groundwaters (Fig. 4) broadly show a scatter plot dominated by a Chloride-Sodium facies. However, when going into small details, the widespread chemical facies of the Phr aquifer is closer to the NaCl pole than those of Cl and CT aquifers. The facies of the Phreatic aquifer most concentrated samples are in the following order: Ca-sulfate < Na-sulfate = Mg-sulfate < Na-chloride. This se-

[Title Page](#)[Abstract](#)[Introduction](#)[Conclusions](#)[References](#)[Tables](#)[Figures](#)[◀](#)[▶](#)[◀](#)[▶](#)[Back](#)[Close](#)[Full Screen / Esc](#)[Printer-friendly Version](#)[Interactive Discussion](#)

quential order of solutes is comparable to that of other groundwater occurring in North Africa, and especially in the neighboring area of the chotts (depressions where salts concentrate by evaporation) Merouane and Melrhir (Vallès et al., 1997; Hamdi-Aïssa et al., 2004).

### 5    3.2 Spatial distribution of the mineralization

The salinity of the phreatic aquifer varies considerably depending on the location (near wells or drains) and time (influence of irrigation; Fig. 5a).

Its salinity is low around irrigated and fairly well-drained areas, such as the palm groves of Hassi Miloud, just north of Ouargla (Fig. 3) that benefit from freshwater and  
10 are drained to the sebkha Oum el Raneb. However, the three lowest salinity values are observed in the wells of Ouargla palm-grove itself, where the Phr aquifer watertable is deeper than 2 m.

Conversely, the highest salinity waters are found in wells drilled in the chotts and  
15 sebkhas (a sebkha is the central part of a chott where salinity is the largest) Safioun and Oum er Raneb where the aquifer is often shallower than 50 cm.

The salinity of the Complexe Terminal (Mio-pliocene) aquifer (Fig. 5b) is much lower than that of the Phr aquifer, and ranges from 1 to  $2 \text{ g L}^{-1}$ ; however, its hardness is larger and it contains more sulfate, chloride and sodium than the waters of the Senonian formations and those of the CI aquifer. The salinity of the Senonian aquifer ranges from  
20 1.1 to  $1.7 \text{ g L}^{-1}$ , while the average salinity of the Continental Intercalaire is  $0.7 \text{ g L}^{-1}$  (Fig. 5c).

A likely contamination of the Mio-pliocene aquifer by phreatic groundwaters through casing leakage in an area where water is heavily loaded with salt and therefore particularly aggressive cannot be excluded.

<a href="#">Title Page</a>	
<a href="#">Abstract</a>	<a href="#">Introduction</a>
<a href="#">Conclusions</a>	<a href="#">References</a>
<a href="#">Tables</a>	<a href="#">Figures</a>
<a href="#">◀</a>	<a href="#">▶</a>
<a href="#">◀</a>	<a href="#">▶</a>
<a href="#">Back</a>	<a href="#">Close</a>
<a href="#">Full Screen / Esc</a>	
<a href="#">Printer-friendly Version</a>	
<a href="#">Interactive Discussion</a>	

### 3.3 Saturation Indices

The calculated saturation indices reveal that waters from CI at 50 °C are close to equilibrium with respect to calcite (Figs. 6 top and 7), except for 3 samples that are slightly oversaturated. They are however all undersaturated with respect to gypsum (Figs. 6 bottom and 8).

Moreover, they are oversaturated with respect to dolomite and undersaturated with respect to anhydrite (Fig. 8) and halite (Fig. 9).

Waters from CT and phreatic aquifers show the same pattern, but some of them are more largely oversaturated with respect to calcite, at 25 °C (Fig. 7).

However, several phreatic waters (P031, P566, PLX4, PL18, P002, P023, P116, P066, P162 and P036) that are located in the sebkhas of Sefioune, Oum-er-Raneb, Bamendil and Ain el Beida's chott are saturated with gypsum and anhydrite. This is in accordance with high evaporative environments found elsewhere (UNESCO, 1972; Hamdi-Aïssa et al., 2004; Slimani, 2006).

No significant saturation indices' evolution from the south to the north upstream and downstream of Oued Mya (Fig. 8) is observed. This suggests that the acquisition of mineralization is due to geochemical processes that have already reached equilibrium or steady state in the upstream areas of Ouargla.

### 3.4 Change of facies from the carbonated pole to the evaporites' pole

The facies shifts progressively from the carbonated (CI and CT aquifers) to the evaporites'one (Phr aquifer) with an increase in sulfates and chlorides at the expense of carbonates (SI of gypsum, anhydrite and halite). This is illustrated by a decrease of the following two ratios:  $[\text{HCO}_3^-] / ([\text{Cl}^-] + 2[\text{SO}_4^{2-}])$ ; Fig. 10) from 0.2 to 0 and of the ratio  $[\text{SO}_4^{2-}] / [\text{Cl}^-]$  from 0.8 to values ranging from 0.3 and 0 (Fig. 11) while salinity increases. Carbonate concentrations tend towards very small values, while it is not the case for sulfates. This is due to both gypsum dissolution and calcite precipitation.

<a href="#">Title Page</a>	
<a href="#">Abstract</a>	<a href="#">Introduction</a>
<a href="#">Conclusions</a>	<a href="#">References</a>
<a href="#">Tables</a>	<a href="#">Figures</a>
<a href="#">◀</a>	<a href="#">▶</a>
<a href="#">◀</a>	<a href="#">▶</a>
<a href="#">Back</a>	<a href="#">Close</a>
<a href="#">Full Screen / Esc</a>	
<a href="#">Printer-friendly Version</a>	
<a href="#">Interactive Discussion</a>	

Chlorides in groundwater may come from three different sources: (i) ancient sea water entrapped in sediments; (ii) dissolution of halite and related minerals that are present in evaporite deposits and (iii) dissolution of dry fallout from the atmosphere, particularly in these arid regions (Matiatos et al., 2014; Hadj-Ammar et al., 2014).

5 For most of the sampled points the  $[Na^+]/[Cl^-]$  ratio remains close to 1, but significant ranges are observed: from 0.85 to 1.26 for Cl aquifer, from 0.40 to 1.02 for the CT aquifer and from 0.13 to 2.15 for the Phr aquifer. All the measured points from the three considered aquifers are more or less linearly scattered around the unity slope straight line that stands for halite dissolution (Fig. 12). The latter appears as the most dominant reaction occurring in the medium. However, at very high salinity,  $Na^+$  seems to swerve 10 from the straight line, towards smaller values.

A further scrutiny of (Fig. 12) shows that Cl waters are very close to the 1 : 1 line. CT waters are enriched in both  $\text{Na}^+$  and  $\text{Cl}^-$  but slightly lower than the 1 : 1 line while phreatic waters are largely enriched and much more scattered. CT waters are closer to the seawater mole ratio (0.858), but some lower values imply a contribution from another source of chloride than halite or from entrapped seawater. Conversely, a  $[\text{Na}^+]/[\text{Cl}^-]$  ratio larger than 1 is observed for phreatic waters, which implies the contribution of another source of sodium, most likely sodium sulfate, that is present as mirabilite or thenardite in the chotts and the sebkhas areas.

[Br<sup>-</sup>] / [Cl<sup>-</sup>] ratio ranges from  $2 \times 10^{-3}$  to  $3 \times 10^{-3}$ . The value of this molar ratio for halite is around  $2.5 \times 10^{-3}$ , which matches the aforementioned range and confirms that halite dissolution is the most dominant reaction taking place in the studied medium.

In these aquifers, calcium originates both from carbonate and sulfate (Figs. 13 and 14). Three samples from Cl aquifer are close to the  $[\text{Ca}^{2+}] / [\text{HCO}_3^-]$  1 : 2 line, while calcium sulfate dissolution explains the excess of calcium. However, a small but significant number of samples (9) from phreatic aquifer are depleted in calcium, and plot under the  $[\text{Ca}^{2+}] / [\text{HCO}_3^-]$  1:2 line. This cannot be explained by precipitation of calcite, as some are undersaturated with respect to that mineral, while others are oversaturated.

<a href="#">Title Page</a>	
<a href="#">Abstract</a>	<a href="#">Introduction</a>
<a href="#">Conclusions</a>	<a href="#">References</a>
<a href="#">Tables</a>	<a href="#">Figures</a>
<a href="#">◀</a>	<a href="#">▶</a>
<a href="#">◀</a>	<a href="#">▶</a>
<a href="#">Back</a>	<a href="#">Close</a>
<a href="#">Full Screen / Esc</a>	
<a href="#">Printer-friendly Version</a>	
<a href="#">Interactive Discussion</a>	

In this case, a cation exchange process seems to occur leading to a preferential adsorption of divalent cations, with a release of  $\text{Na}^+$ . This is confirmed by the inverse modeling that is developed below and which implies  $\text{Mg}^{2+}$  fixation and  $\text{Na}^+$  and  $\text{K}^+$  releases.

Larger sulfate values observed in the phreatic aquifer (Fig. 14) with  $[\text{Ca}^{2+}]/[\text{SO}_4^{2-}] < 1$  can be attributed to a sodium-magnesium sulfate dissolution from a mineral bearing such elements. This is for instance the case of bloedite.

### 3.5 Isotope geochemistry

CT and CI aquifer exhibit depleted and homogeneous  $^{18}\text{O}$  contents, ranging from  $-8.32\text{ ‰}$  to  $-7.85\text{ ‰}$ . This was already previously reported by many authors (Edmunds et al., 2003; Guendouz et al., 2003; Moulla et al., 2012). On the other hand,  $^{18}\text{O}$  values for the phreatic aquifer are widely dispersed and vary between  $-8.84$  to  $3.42\text{ ‰}$  (Table 6).

Waters located north of the Hassi Miloud to Sebkhet Saifioune axis are more enriched in heavy isotopes and therefore more evaporated. In that area, water table is close to the surface and mixing of both CI and CT groundwaters with phreatic ones through irrigation is nonexistent. Conversely, waters located south of Hassi Miloud up to Ouargla city show depleted values. This is the clear fingerprint of a contribution to the Phr waters from the underlying CI and CT aquifers (Gonfiantini et al., 1975; Guendouz, 1985; Fontes et al., 1986; Guendouz and Moulla, 1996).

Phreatic waters result from a mixing of two end-members. An evidence for this is given by considering the ( $[\text{Cl}^-]$ ,  $^{18}\text{O}$ ) relationship (Fig. 15). The two poles are: (i) a first pole of  $^{18}\text{O}$  depleted groundwater (Fig. 16), and (ii) another pole of  $^{18}\text{O}$  enriched groundwater with positive values and a high salinity. The latter is composed of phreatic waters occurring in the northern part of the study region.

Pole I represents the waters from CI and CT whose isotopic composition is depleted in  $^{18}\text{O}$  (average value around  $-8.2\text{ ‰}$ ; Fig. 15). They correspond to an old water recharge (palæorecharge); whose age estimated by means of  $^{14}\text{C}$ , exceeds 15 000 years BP (Guendouz, 1985; Guendouz and Michelot, 2006). So, it is not a water

body that is recharged by recent precipitation. It consists of Cl and CT groundwaters and partly of phreatic waters, and can be ascribed to an upward leakage favored by the extension of faults near Amguid El-Biod dorsal.

Pole II, observed in Sebkhet Safioune, can be ascribed to the direct dissolution of 5 superficial evaporitic deposits conveyed by evaporated rainwater.

Evaporation alone cannot explain the distribution of data that is observed (Fig. 15). An evidence for this is given in a semi-logarithmic plot (Fig. 16), as classically obtained according to the simple approximation of Rayleigh equation (cf. Appendix):

$$\delta^{18}\text{O} \approx 1000 \times (1 - \alpha) \log[\text{Cl}^-] + \text{cte}, \quad (1)$$

$$10 \approx -\epsilon \log[\text{Cl}^-] + \text{cte}, \quad (2)$$

where  $\alpha$  is the fractionation factor during evaporation, and  $\epsilon \equiv -1000 \times (1 - \alpha)$  is the enrichment factor, and cte is an abbreviation for constant (Ma et al., 2010; Chkir et al., 2009).

CI and CT waters are better separated in the semi-logarithmic plot because they are 15 differentiated by their chloride content. According to Eq. (1), simple evaporation gives a straight line (solid line in Fig. 16). The value of  $\epsilon$  used is the value at 25 °C, which is equal to -73.5. There is only one sample (P115) on the evaporation straight line, which could be considered as an outlier in Fig. 15 ( $[\text{Cl}^-] \approx 0$ ). All other samples fit on the logarithmic curve derived from the mixing line illustrated by Fig. 15.

The phreatic waters that are close to pole I (Fig. 15) correspond to groundwaters 20 occurring in the edges of the basin (Hassi Miloud, piezometer P433; Fig. 16). They are low-mineralized and acquire their salinity via two processes namely: dissolution of evaporites along their underground transit up to Sebkhet Safioune and dilution through upward leakage by the less-mineralized waters of Cl and CT aquifers (for example Hedeb I for Cl and D7F4 for CT; Fig. 16; Guendouz, 1985; Guendouz and Moulla, 25 1996).

[Title Page](#)[Abstract](#)[Introduction](#)[Conclusions](#)[References](#)[Tables](#)[Figures](#)[◀](#)[▶](#)[◀](#)[▶](#)[Back](#)[Close](#)[Full Screen / Esc](#)[Printer-friendly Version](#)[Interactive Discussion](#)

The rates of the mixing that are due to upward leakage from Cl to CT towards the phreatic aquifer can be calculated by means of a mass balance equation. It only requires knowing the  $\delta$  values of each fraction that is involved in the mixing process.

The  $\delta$  value of the mixture is given by:

$$^5 \quad \delta_{\text{mix}} = f_1 \times \delta_1 + f_2 \times \delta_2 \quad (3)$$

where  $f_1$  is the fraction of Cl aquifer,  $f_2$  the fraction of the CT and  $\delta_1$ ,  $\delta_2$  are the respective isotope contents.

Average values of mixing fractions from each aquifer to the phreatic waters computed by means of Eq. (3) gave the rates of 65 % for Cl aquifer and 35 % for CT aquifer.

A mixture of a phreatic water component that is close to pole I (i.e. P433) with another one which is rather close to pole II (i.e. P039; Figs. 15 and 16), for an intermediate water with a  $\delta^{18}\text{O}$  signature ranging from  $-5$  to  $-2\text{\textperthousand}$  gives mixture fraction values of 52 % for pole I and 48 % for pole II. Isotope results will be used to independently cross-check the validity of the mixing fractions derived from an inverse modeling involving chemical data (cf. infra).

Turonian evaporites are found to lie in between Cl deep aquifer, and the Senonian and Miocene formations bearing CT aquifer. CT waters can thus simply originate from ascending Cl waters that dissolve Turonian evaporites, a process which does not involve any change in  $^{18}\text{O}$  content. Conversely, phreatic waters result to a minor degree from evaporation, and mostly from dissolution of sebkhas evaporites by  $^{18}\text{O}$  enriched rainwater and mixing with Cl-CT waters.

### 3.5.1 Tritium content of water

Tritium contents of Phr aquifer are relatively small (Table 6), they vary between 0 and 8 TU. Piezometers PZ12, P036 and P068 show values close to 8 TU, piezometers P018, P019, P416, P034, P042 and P093 exhibit values ranging between 5 and 6 TU, and the rest of the samples' concentrations are lower than 2 TU. The comparison of

[Title Page](#)

[Abstract](#)

[Introduction](#)

[Conclusions](#)

[References](#)

[Tables](#)

[Figures](#)

◀

▶

◀

▶

[Back](#)

[Close](#)

[Full Screen / Esc](#)

[Printer-friendly Version](#)

[Interactive Discussion](#)



these results with that of precipitation which was 16 TU in 1992 suggests the existence of a mixture of water infiltrated before 1950 and a more recent one corresponding to the 1980s (Guendouz and Moulla, 1996; Edmunds et al., 2003; Guendouz et al., 2003; Moulla et al., 2012; ONM, 1975/2013). This is in agreement with the recorded hydrochemical and stable isotope data.

### 3.6 Inverse modeling

We assume that the relationship between  $^{18}\text{O}$  and Cl $^-$  data obtained in 1996 is stable with time, which is a logical assumption as times of transfer from Cl to both CT and Phr are very long. Considering both  $^{18}\text{O}$  and Cl $^-$  data, thus Cl, CT and Phr data populations can be categorized as follows:

- Cl does not show appreciable  $^{18}\text{O}$  variations. Its data can be considered as a single population;
- the same holds for CT;
- Phr samples consist however of different populations:
  - pole I, with  $\delta^{18}\text{O}$  values close to -8, and small Cl $^-$  concentrations, more specifically less than 35 mmol L $^{-1}$  (Fig. 17);
  - pole II, with  $\delta^{18}\text{O}$  values larger than 3, and very large Cl $^-$  concentrations, more specifically larger than 4000 mmol L $^{-1}$  (Fig. 17);
  - intermediate Phr samples resulting from mixing between poles I and II (mixing line in Fig. 15, mixing curve in Fig. 16);
  - intermediate samples resulting from evaporation of pole I (evaporation line in Fig. 16).

Statistical parameters for Cl, CT, Phr pole I and Phr pole II are given in Table 7.

<a href="#">Title Page</a>	
<a href="#">Abstract</a>	<a href="#">Introduction</a>
<a href="#">Conclusions</a>	<a href="#">References</a>
<a href="#">Tables</a>	<a href="#">Figures</a>
<a href="#">◀</a>	<a href="#">▶</a>
<a href="#">◀</a>	<a href="#">▶</a>
<a href="#">Back</a>	<a href="#">Close</a>
<a href="#">Full Screen / Esc</a>	
<a href="#">Printer-friendly Version</a>	
<a href="#">Interactive Discussion</a>	

The mass-balance modeling has shown that relatively few phases are required to derive observed changes in water chemistry and to account for the hydrochemical evolution in Ouargla's region. The mineral phases' selection is based upon geological descriptions and analysis of rocks and sediments from the area (OSS, 2003; Hamdi-Aïssa et al., 2004).

The inverse model was constrained so that mineral phases from evaporites including gypsum, halite, mirabilite, gлаuberite, sylvite and bloedite were set to dissolve until they reach saturation, and calcite, dolomite were set to precipitate once they reached saturation. Cation exchange reactions of  $\text{Ca}^{2+}$ ,  $\text{Mg}^{2+}$ ,  $\text{K}^+$  and  $\text{Na}^+$  on exchange sites were included in the model to check which cations are adsorbed or desorbed during the process. Dissolution and desorption contribute as positive terms in the mass balance, as elements are released in solution. On the other hand, precipitation and adsorption contribute as negative terms, while elements removed from the solution.  $\text{CO}_{2(g)}$  dissolution is considered by Phreeqc as a dissolution of a mineral, whereas  $\text{CO}_{2(g)}$  degassing is dealt with as if it were a mineral precipitation.

Inverse modelling leads to a quantitative assessment of the different solutes' acquisition processes and a mass balance for the salts that are dissolved or precipitated from Cl, CT and Phr groundwaters (Fig. 16, Table 8), as follows:

- 20 – transition from CI to CT involves gypsum, halite and sylvite dissolution, and some ion exchange namely calcium and potassium fixation on exchange sites against magnesium release, with a very small and quite negligible amount of  $\text{CO}_{2(g)}$  de-gassing. The maximum elemental concentration fractional error equals 1 %. The model consists of a minimum number of phases (i.e. 6 solid phases and  $\text{CO}_{2(g)}$ ); Another model implies as well dolomite precipitation with the same fractional error;

25 – transition from CT to an average water component of pole I involves dissolution of halite, sylvite, and bloedite from Turonian evaporites, with a very tiny calcite precipitation. The maximum fractional error in elemental concentration is 4 %. An-

other model implies  $\text{CO}_{2(g)}$  escape from the solution, with the same fractional error. Large amounts of  $\text{Mg}^{2+}$  and  $\text{SO}_4^{2-}$  are released within the solution (Sharif et al., 2008; Li et al., 2010; Carucci et al., 2012);

- the formation of Phr pole II can be modeled as being a direct dissolution of salts from the sebkha by rainwater with positive  $\delta^{18}\text{O}$ ; the most concentrated water (P036 from Sebkhet Safioune) is taken here for pole II, and pure water as rainwater. In a decreasing order of amounts respectively involved in that process, halite, sylvite, gypsum and huntite dissolve, and little calcite precipitates while some  $\text{Mg}^{2+}$  are released vs.  $\text{K}^+$  fixation on exchange sites. The maximum elemental fractional error in the concentration is equal to 0.004 %. Another model implies dolomite precipitation with some more huntite dissolving, instead of calcite precipitation, but salt dissolution and ion exchange are the same. Huntite, dolomite and calcite stoichiometries are linearly related, so both models can fit field data, but calcite precipitation is preferred compared to dolomite precipitation at low temperature;
- the origin of all phreatic waters can be explained by a mixing in variable proportions of pole I and pole II. For instance, waters from pole I and pole II can easily be separated by their  $\delta^{18}\text{O}$  respectively close to  $-8$  and  $+3.5\text{\textperthousand}$  (Figs. 15 and 16). Mixing the two poles is of course not an inert reaction, but rather results in the dissolution and the precipitation of minerals. Inverse modeling is then used to compute both mixing rates and the extent of matter exchange between soil and solution. For example, a phreatic water (piezometer P068) with intermediate values ( $\delta^{18}\text{O} = -3$  and  $[\text{Cl}^-] \simeq 2M$ ) is explained by the mixing of 58 % water from pole I and 42 % from pole II. In addition, calcite precipitates,  $\text{Mg}^{2+}$  fixes on exchange sites, against  $\text{Na}^+$  and  $\text{K}^+$ , gypsum dissolves as well as a minor amount of huntite (Table 8). The maximum elemental concentration fractional error is 2.5 % and the mixing fractions' weighted the  $\delta^{18}\text{O}$  is  $-3.17\text{\textperthousand}$ , which is very close to the measured value ( $-3.04\text{\textperthousand}$ ). All the other models, making use

## Chemical and isotopic data from groundwaters in Sahara

R. Slimani et al.

[Title Page](#)

[Abstract](#)

[Introduction](#)

[Conclusions](#)

[References](#)

[Tables](#)

[Figures](#)

[◀](#)

[▶](#)

[◀](#)

[▶](#)

[Back](#)

[Close](#)

[Full Screen / Esc](#)

[Printer-friendly Version](#)

[Interactive Discussion](#)



of a minimum number of phases, and not taking into consideration ion exchange reactions are not found compatible with isotope data. Mixing rates obtained with such models are for example 98 % of pole I and 0.9 % of pole II, which leads to a  $\delta^{18}\text{O} = (-7.80\text{\textperthousand})$  which is quite far for the real measured value ( $-3.04\text{\textperthousand}$ ).

- 5 The main types of groundwaters occurring in Ouargla basin are thus explained and could quantitatively be reconstructed. An exception is however sample P115, which is located exactly on the evaporation line of Phr pole I. Despite numerous attempts, it could not be quantitatively rebuilt. Its  ${}^3\text{H}$  value (6.8) indicates that it is derived from a more or less recent water component with very small salt content, most possibly  
10 affected by rainwater and some preferential flow within the piezometer. As this is the only sample on this evaporation line, there remains a doubt on its significance.

Globally, the summary of mass transfer reactions occurring in the studied system (Table 8) shows that gypsum dissolution results in calcite precipitation and  $\text{CO}_{2(g)}$  dissolution, thus acting as an inorganic carbon sink.

## 15 4 Conclusions

Groundwater hydrochemistry is a good record indicator for the water-rock interactions that occur along the groundwater flowpath. The mineral load reflects well the complex processes taking place while water circulates underground since its point of infiltration.

- The hydrochemical study of the aquifer system occurring in Ouargla's basin allowed  
20 us to identify the origin of its mineralization. Waters exhibit two different facies: sodium chloride and sodium sulfate for the phreatic aquifer (Phr), sodium sulfate for the Complexe Terminal (CT) aquifer and sodium chloride for the Continental Intercalaire (CI) aquifer. Calcium carbonate precipitation and evaporite dissolution explain the facies change from carbonate to sodium chloride or sodium sulfate. However reactions imply many minerals with common ions, deep reactions without evaporation as well as shallow processes affected by both evaporation and mixing. Those processes are sep-  
25

<a href="#">Title Page</a>	
<a href="#">Abstract</a>	<a href="#">Introduction</a>
<a href="#">Conclusions</a>	<a href="#">References</a>
<a href="#">Tables</a>	<a href="#">Figures</a>
<a href="#">◀</a>	<a href="#">▶</a>
<a href="#">◀</a>	<a href="#">▶</a>
<a href="#">Back</a>	<a href="#">Close</a>
<a href="#">Full Screen / Esc</a>	
<a href="#">Printer-friendly Version</a>	
<a href="#">Interactive Discussion</a>	



arated by considering both chemical and isotopic data, and quantitatively explained making use of an inverse geochemical modeling.

The main result is that Phr waters do not originate simply from infiltration of rainwater and dissolution of salts from the sebkhas. Conversely, Phr waters are largely influenced by the upwardly mobile deep CT and Cl groundwaters, fractions of the latter interacting with evaporites from Turonian formations. Phreatic waters occurrence is explained as a mixing of two end-member components: pole I, which is very close to Cl and CT, and pole II, which is highly mineralized and results from the dissolution by rainwater of salts from the sebkhas.

At depth, Cl leaks upwardly and dissolves gypsum, halite and sylvite, with some ion exchange, to give waters of CT aquifer composition.

CT transformation into Phr pole I waters involves the dissolution of Turonian evaporites (halite, sylvite and bloedite) with minor calcite precipitation.

At the surface, direct dissolution by rainwater of salts from sebkhas (halite, sylvite, gypsum and some huntite) with precipitation of calcite and  $Mg^{2+}/K^+$  ion exchange results in pole II Phr composition.

All phreatic groundwaters result from a mixing of pole I and pole II water that is accompanied by calcite precipitation, fixation of  $Mg^{2+}$  on ion exchange sites against the release of  $K^+$  and  $Na^+$ .

Moreover, some  $CO_{2(g)}$  escapes from the solution at depth, but dissolves much more at the surface. The most complex phenomena occur during the dissolution of Turonian evaporites while Cl leaks upwardly towards CT, and from Phr I to Phr II, while the transition from CT to Phr I implies a very limited number of phases. Globally, gypsum dissolution and calcite precipitation processes both act as an inorganic carbon sink.

## Chemical and isotopic data from groundwaters in Sahara

R. Slimani et al.

[Title Page](#)

[Abstract](#)

[Introduction](#)

[Conclusions](#)

[References](#)

[Tables](#)

[Figures](#)

[◀](#)

[▶](#)

[◀](#)

[▶](#)

[Back](#)

[Close](#)

[Full Screen / Esc](#)

[Printer-friendly Version](#)

[Interactive Discussion](#)



## Appendix A

According to a simple Rayleigh equation, the evolution of the heavy isotope ratio in the remaining liquid  $R_l$  is given by:

$$R_l \approx R_{l,0} \times f_l^{\alpha-1}, \quad (A1)$$

where  $f_l$  is the fraction remaining liquid and  $\alpha$  the fractionation factor.

The fraction remaining liquid is derived from chloride concentration, as chloride can be considered as conservative during evaporation: all phreatic waters are undersaturated with respect to halite, that precipitates only in the last stage. Hence, the following equation holds:

$$f_l \equiv \frac{n_{w,1}}{n_{w,0}} = \frac{[\text{Cl}^-]_0}{[\text{Cl}^-]_1}. \quad (A2)$$

By taking natural logarithms, one obtains:

$$\ln R_l \approx (1 - \alpha) \times \ln [\text{Cl}^-] + \text{cte}, \quad (A3)$$

As, by definition,

$$R_l \equiv R_{\text{std.}} \times \left(1 + \frac{\delta^{18}\text{O}}{1000}\right), \quad (A4)$$

one has:

$$\ln R_l \equiv \ln R_{\text{std.}} + \ln \left(1 + \frac{\delta^{18}\text{O}}{1000}\right), \quad (A5)$$

$$\approx \ln R_{\text{std.}} + \frac{\delta^{18}\text{O}}{1000}, \quad (A6)$$

Title Page

Abstract

Introduction

Conclusions

References

Tables

Figures

◀

▶

◀

▶

Back

Close

Full Screen / Esc

Printer-friendly Version

Interactive Discussion



hence, with base 10 logarithms:

$$\delta^{18}\text{O} \approx 1000(1 - \alpha) \log[\text{Cl}^-] + \text{cte}, \quad (\text{A7})$$

$$\approx -\epsilon \log[\text{Cl}^-] + \text{cte}, \quad (\text{A8})$$

where as classically defined  $\epsilon = 100(\alpha - 1)$  is the enrichment factor.

- 5 *Acknowledgements.* The authors wish to thank the staff members of the National Agency for Water Resources in Ouargla (ANRH) and the Laboratory of Algerian waters (ADE) for the support provided to the Technical Cooperation within which this work was carried out. Analyses of  $^{18}\text{O}$  were funded by the project CDTN/DDHI (Guendouz and Moulla, 1996). The supports of University of Ouargla and of INRA for travel grants of R. Slimani and G. Bourrié are gratefully acknowledged too.
- 10

## References

- AI-Gamal, S. A.: An assessment of recharge possibility to North-Western Sahara Aquifer System (NWSAS) using environmental isotopes, *J. Hydrol.*, 398, 184–190, 2011. 3
- ANRH: Inventaire des forages de la Wilaya de Ouargla, Rapport technique, Agence Nationale des Ressources Hydrauliques, 2011. 5
- Aumassip, G., Dagorne, A., Estorges, P., Lefèvre-Witier, P., Mahroud, F., Nesson, C., Rouvillois-Brigol, M., and Trecolle, G.: Aperçus sur l'évolution du paysage quaternaire et le peuplement de la région de Ouargla, Libyca, 205–257, 1972. 4
- Belkhiri, L., Boudoukha, A., Mouni, L., and Baouz, T.: Application of multivariate statistical methods and inverse geochemical modeling for characterization of groundwater – A case study: Ain Azel plain (Algeria), *Geoderma*, 159, 390–398, 2010. 6
- Belkhiri, L., Mouni, L., and Boudoukha, A.: Geochemical evolution of groundwater in an alluvial aquifer: Case of El Eulma aquifer, East Algeria, *Journal of African Earth Sciences*, 66–67, 46–55, 2012. 6
- Carucci, V., Petitta, M., and Aravena, R.: Interaction between shallow and deep aquifers in the Tivoli Plain (Central Italy) enhanced by groundwater extraction: A

<a href="#">Title Page</a>	
<a href="#">Abstract</a>	<a href="#">Introduction</a>
<a href="#">Conclusions</a>	<a href="#">References</a>
<a href="#">Tables</a>	<a href="#">Figures</a>
<a href="#">◀</a>	<a href="#">▶</a>
<a href="#">◀</a>	<a href="#">▶</a>
<a href="#">Back</a>	<a href="#">Close</a>
<a href="#">Full Screen / Esc</a>	
<a href="#">Printer-friendly Version</a>	
<a href="#">Interactive Discussion</a>	



## Chemical and isotopic data from groundwaters in Sahara

R. Slimani et al.

[Title Page](#)

[Abstract](#)

[Introduction](#)

[Conclusions](#)

[References](#)

[Tables](#)

[Figures](#)

[◀](#)

[▶](#)

[◀](#)

[▶](#)

[Back](#)

[Close](#)

[Full Screen / Esc](#)

[Printer-friendly Version](#)

[Interactive Discussion](#)



- multi-isotope approach and geochemical modeling, *Appl. Geochem.*, 27, 266–280, doi:10.1016/j.apgeochem.2011.11.007, 2012. 15
- Chellat, S., Bourefis, A., Hamdi-Aïssa, B., and Djerrab, A.: Paleoenvironmental reconstitution of Mio-pliocene sandstones of the lower-Sahara at the base of exoscopic and sequential analysis, *Pensee Journal*, 76, 34–51, 2014. 4
- Chkhir, N., Guendouz, A., Zouari, K., Hadj Ammar, F., and Moulla, A.: Uranium isotopes in groundwater from the continental intercalaire aquifer in Algerian Tunisian Sahara (Northern Africa), *Journal of Environmental Radioactivity*, 100, 649–656, doi:10.1016/j.jenvrad.2009.05.009, 2009. 11
- Cornet, A. and Gouscov, N.: Les eaux du Crétacé inférieur continental dans le Sahara algérien: nappe dite “Albien”, in: *Congrès géologique international*, vol. tome II, p. 30, Alger, 1952. 3, 4
- Deutsch, W.: *Groundwater Chemistry-Fundamentals and Applications to Contamination*, New York, 1997. 6
- Dubief, J.: *Essai sur l'hydrologie superficielle au Sahara*, Direction du service de la colonisation et de l'hydraulique, Service des études scientifiques, 1953. 4
- Dubief, J.: *Le climat du Sahara*, Hors-série, Institut de recherches sahariennes, 1963. 4
- Eckstein, G. and Eckstein, Y.: A hydrogeological approach to transboundary ground water resources and international law, *American University International Law Review*, 19, 201–258, 2003. 2
- Edmunds, W., Guendouz, A., Mamou, A., Moulla, A., Shand, P., and Zouari, K.: Groundwater evolution in the continental intercalaire aquifer of southern Algeria and Tunisia: trace element and isotopic indicators, *Appl. Geochem.*, 18, 805–822, 2003. 3, 10, 13
- Fontes, J., Yousfi, M., and Allison, G.: Estimation of long-term, diffuse groundwater discharge in the northern Sahara using stable isotope profiles in soil water, *J. Hydrol.*, 86, 315–327, 1986. 3, 10
- Foster, S., Margat, J., and Droubi, A.: Concept and importance of nonrenewable resources, no. 10 in IHP-VI Series on Groundwater, UNESCO, 2006. 3
- Gonfiantini, R., Conrad, G., Fontes, J.-C., Sauzay, G., and Payne, B.: Étude isotopique de la nappe du Continental Intercalaire et de ses relations avec les autres nappes du Sahara septentrional, *Isotope Techniques in Groundwater Hydrology*, 1, 227–241, 1975. 10
- Grenthe, I. and Plyasunov, A.: On the use of semiempirical theories for the modeling of solution chemical data, *Pure and Applied Chemistry*, 69, 951–958, 1997. 4

- Guendouz, A.: Contribution à l'étude hydrochimique et isotopique des nappes profondes du Sahara nord-est septentrional, Algérie, Phd thesis, Université d'Orsay, France, 1985. 3, 10, 11
- Guendouz, A. and Michelot, J.: Chlorine-36 dating of deep groundwater from northern Sahara, 5 J. Hydrol., 328, 572–580, 2006. 10
- Guendouz, A. and Moulla, A.: Étude hydrochimique et isotopique des eaux souterraines de la cuvette de Ouargla, Algérie, Rapport technique, CDTN/DDHI, 1996. 3, 5, 10, 11, 13, 19
- Guendouz, A., Moulla, A., Edmunds, W., Zouari, K., Shands, P., and Mamou, A.: Hydrogeochemical and isotopic evolution of water in the complex terminal aquifer in Algerian Sahara, 10 Hydrogeol. J., 11, 483–495, 2003. 3, 10, 13
- Guler, C. and Thyne, G.: Hydrologic and geologic factors controlling surface and groundwater chemistry in Indian wells Owens valley area, southeastern California, USA, J. Hydrol., 285, 177–198, 2004. 6
- Hadj-Ammar, F., Chkir, N., Zouari, K., Hamelin, B., Deschamps, P., and Aigoun, A.: Hydrogeochemical processes in the Complexe Terminal aquifer of southern Tunisia: An integrated investigation based on geochemical and multivariate statistical methods, Journal of African Earth Sciences, 100, 81–95, doi:10.1016/j.jafrearsci.2014.06.015, 2014. 9
- Hamdi-Aïssa, B., Vallès, V., Aventurier, A., and Ribolzi, O.: Soils and brines geochemistry and mineralogy of hyper arid desert playa, Ouargla basin, Algerian Sahara, Arid Land Research and Management, 18, 103–126, 2004. 3, 7, 8, 14
- Kenoyer, G. and Bowser, C.: Groundwater chemical evolution in a sandy aquifer in northern Wisconsin, Water Resour. Res., 28, 591–600, 1992. 6
- Kuells, C., Adar, E., and Udluft, P.: Resolving patterns of ground water flow by inverse hydrochemical modeling in a semiarid Kalahari basin, Tracers and Modelling in Hydrogeology, 262, 25 447–451, 2000. 6
- Le Houérou, H.: Bioclimatology and biogeography of Africa, Springer Verlag, 2009. 4
- Lelièvre, R.: Assainissement de la cuvette de Ouargla, rapports géohydraulique no 2, Ministère des Travaux Publics et de la construction, 1969. 5
- Li, P., Qian, H., Wu, J., and Ding, J.: Geochemical modeling of groundwater in southern plain area of Pengyang County, Ningxia, China, Water Science and Engineering, 3, 282–291, 30 2010. 15

## Chemical and isotopic data from groundwaters in Sahara

R. Slimani et al.

[Title Page](#)

[Abstract](#)

[Introduction](#)

[Conclusions](#)

[References](#)

[Tables](#)

[Figures](#)

[◀](#)

[▶](#)

[◀](#)

[▶](#)

[Back](#)

[Close](#)

[Full Screen / Esc](#)

[Printer-friendly Version](#)

[Interactive Discussion](#)



- Ma, J., Pan, F., Chen, L., Edmunds, W., Ding, Z., Zhou, K., He, J., Zhoua, K., and Huang, T.: Isotopic and geochemical evidence of recharge sources and water quality in the Quaternary aquifer beneath Jinchang city, NW China, *Appl. Geochem.*, 25, 996–1007, 2010. 11
- Matiatos, I., Alexopoulos, A., and Godelitsas, A.: Multivariate statistical analysis of the hydrogeochemical and isotopic composition of the groundwater resources in northeastern Peloponnesus (Greece), *Sci. Total Environ.*, 476–477, 577–590, doi:10.1016/j.scitotenv.2014.01.042, 2014. 9
- Moulias, D.: *L'eau dans les oasis sahariennes, organisation hydraulique, régime juridique*, PhD thesis, Alger, 1927. 5
- Moulla, A., Guendouz, A., Cherchali, M.-H., Chaid, Z., and Ouarezki, S.: Updated geochemical and isotopic data from the Continental Intercalaire aquifer in the Great Occidental Erg sub-basin (south-western Algeria), *Quaternary International*, 257, 64–73, 2012. 10, 13
- OECD: *OECD Environmental Outlook to 2030*, Tech. Rep. 1, Organisation for Economic Cooperation and Development, 2008. 2
- ONM: Bulletins mensuels de relevé des paramètres climatologiques en Algérie, Office national météorologique, 1975/2013. 4, 13
- OSS: Système aquifère du Sahara septentrional, Tech. rep., Observatoire du Sahara et du Sahel, 2003. 2, 14
- OSS: Système aquifère du Sahara septentrional (Algérie, Tunisie, Libye): gestion concertée d'un bassin transfrontalier, Tech. Rep. 1, Observatoire du Sahara et du Sahel, 2008. 2, 3
- Ould Baba Sy, M. and Besbes, M.: Holocene recharge and present recharge of the Saharan aquifers – a study by numerical modeling, in: *International symposium – Management of major aquifers*, 2006. 4
- Parkhurst, D. and Appelo, C.: Description of Input and Examples for PHREEQC (Version 3) – A computer program for speciation, batch-reaction, one-dimensional transport, and inverse geochemical calculations, Tech. Rep. 6, U.S. Department of the Interior, U.S. Geological Survey, <http://pubs.usgs.gov/tm/06/a43> (last access: 29 January 2016), 2013. 4, 5, 6, 31
- Plummer, L. and Back, M.: The mass balance approach: application to interpreting the chemical evolution of hydrological systems, *Am. J. Sci.*, 280, 130–142, 1980. 6
- Plummer, L. and Sprinkle, C.: Radiocarbon dating of dissolved inorganic carbon in groundwater from confined parts of the upper Floridan aquifer, Florida, USA, *J. Hydrol.*, 9, 127–150, 2001. 6

## Chemical and isotopic data from groundwaters in Sahara

R. Slimani et al.

[Title Page](#)

[Abstract](#)

[Introduction](#)

[Conclusions](#)

[References](#)

[Tables](#)

[Figures](#)

◀

▶

◀

▶

[Back](#)

[Close](#)

[Full Screen / Esc](#)

[Printer-friendly Version](#)

[Interactive Discussion](#)



- Sharif, M., Davis, R., Steele, K., Kim, B., Kresse, T., and Fazio, J.: Inverse geochemical modeling of groundwater evolution with emphasis on arsenic in the Mississippi River Valley alluvial aquifer, Arkansas (USA), *J. Hydrol.*, 350, 41–55, doi:10.1016/j.jhydrol.2007.11.027, 2008. 15
- 5 Slimani, R.: Contribution à l'évaluation d'indicateurs de pollution environnementaux dans la région de Ouargla: cas des eaux de rejets agricoles et urbaines, Master's thesis, Université de Ouargla, 2006. 3, 8
- Stumm, W. and Morgan, J.: *Aquatic Chemistry: Chemical Equilibria and Rates in Natural Waters*, John Wiley and Sons, 1999. 44, 45, 46
- 10 Thomas, J., Welch, A., and Preissler, A.: Geochemical evolution of ground water in Smith Creek valley – a hydrologically closed basin in central Nevada, USA, *Appl. Geochem.*, 4, 493–510, 1989. 6
- UNESCO: Projet ERESS, Étude des ressources en eau du Sahara septentrional, Tech. Rep. 10, UNESCO, 1972. 2, 3, 8
- 15 Vallès, V., Rezagui, M., Auque, L., Semadi, A., Roger, L., and Zouggari, H.: Geochemistry of saline soils in two arid zones of the Mediterranean basin. I. Geochemistry of the Chott Melghir-Mehrouane watershed in Algeria, *Arid Soil Research and Rehabilitation*, 11, 71–84, 1997. 7

## Chemical and isotopic data from groundwaters in Sahara

R. Slimani et al.

[Title Page](#)

[Abstract](#)

[Introduction](#)

[Conclusions](#)

[References](#)

[Tables](#)

[Figures](#)

◀

▶

◀

▶

[Back](#)

[Close](#)

[Full Screen / Esc](#)

[Printer-friendly Version](#)

[Interactive Discussion](#)



## Chemical and isotopic data from groundwaters in Sahara

R. Slimani et al.

**Table 1.** Field and analytical data for the Continental Intercalaire aquifer.

Locality	Lat.	Long.	Elev.	Date	EC	t	pH	Alk.	Cl <sup>-</sup>	SO <sub>4</sub> <sup>2-</sup>	Na <sup>+</sup>	K <sup>+</sup>	Mg <sup>2+</sup>	Ca <sup>2+</sup>	Br <sup>-</sup>
	m				mS cm <sup>-1</sup>	°C				mmol L <sup>-1</sup>					
Hedeb I	3534750	723986	134.8	09/11/2012	2.01	46.5	7.65	3.5	5.8	6.79	10.7	0.63	2.49	3.3	0.034
Hedeb I	3534750	723986	134.8	1996	1.9	49.3	7.35	0.42	5.81	1.07	5.71	0.18	0.77	0.48	
Hadeb II	3534310	724290	146.2	1996	2.02	47.4	7.64	0.58	6.19	1.22	5.06	0.2	1.28	0.82	
Aouinet Moussa	3548896	721076	132.6	1996	2.2	48.9	7.55	1.28	6.49	1.28	5.65	0.16	1.14	1.17	
Aouinet Moussa	3548896	721076	132.6	22/02/2013	2.2	48.9	7.55	3.19	9.8	3.89	6.3	0.69	5.71	1.27	
Hedeb I	3534750	723986	134.8	11/12/2010	2.19	49.3	7.35	1.91	12.4	4.58	10.7	0.7	3.77	2.35	
Hadeb II	3534310	724290	146.2	11/12/2010	2.26	47.4	7.64	2.11	13.1	5.46	13.9	0.53	4.53	1.41	
Hassi Khifif	3591659.8	721636.5	110	24/02/2013	2.43	50.5	6.83	2.98	14.3	5.24	10.8	0.84	3.44	4.63	0.033
Hedeb I	3534750	723986	134.8	27/02/2013	2.01	46.5	7.65	3.46	15.1	7.67	11.8	0.51	5.57	5.16	
Hassi Khifif	3591659.8	721636.5	110	09/11/2012	2	50.1	7.56	3.31	15.3	7.77	12.2	0.59	5.77	4.95	
El-Bour	3560264	720366	160	22/02/2013	2.96	54.5	7.34	2.58	18.6	6.21	20.6	0.66	4.79	1.38	

- [Title Page](#)
- [Abstract](#) [Introduction](#)
- [Conclusions](#) [References](#)
- [Tables](#) [Figures](#)
- [◀](#) [▶](#)
- [◀](#) [▶](#)
- [Back](#) [Close](#)
- [Full Screen / Esc](#)
- [Printer-friendly Version](#)
- [Interactive Discussion](#)



**Table 2.** Field and analytical data for the Complexe Terminal aquifer.

Locality	Site	Aquifer	Lat.	Long.	Elev.	Date	EC	<i>t</i>	pH	Alk.	Cl <sup>-</sup>	SO <sub>4</sub> <sup>2-</sup>	Na <sup>+</sup>	K <sup>+</sup>	Mg <sup>2+</sup>	Ca <sup>2+</sup>	Br <sup>-</sup>
			m	mS cm <sup>-1</sup>	°C	mmol L <sup>-1</sup>											
Bamendil	D7F4	M	3560759.6	720586.2	296	20/01/2013	2.02	20.1	7.86	1.63	10.1	5.79	9.88	0.68	3.92	2.51	
Bamendil	D7F4	M	3560759.6	720586.2	296	1996	2	21.1	8.2	0.96	10.6	3.54	10.61	0.09	2.33	1.8	
Ifri	D1F151	S	3538891.7	721060.5	204	1996	2.67	23.5	7	1.26	10.75	2.71	7.99	0.73	2.32	2.12	
Said Otba	D2F66	S	3540257.3	720085.4	216	1996	2.31	24	8	1.43	11.02	4.73	11.47	0.16	2.07	3.33	
Oglat Larbaâ	D6F64	M	3566501.4	729369.3	177	1996	2.31	18	7.9	1.41	11.36	6.85	11.59	2.31	1.96	4.58	
El Bour	D4F94	M	3536245.2	722641.7	100.6	27/01/2013	3.05	26.2	7.37	1.61	12.8	6.79	5.15	1.94	1.65	9.13	
Said Otba I	D2F71	S	3574712.4	718272.8	211.9	1996	2.27	24.2	8.2	1.54	13.53	5.72	14.99	0.33	3.28	2.57	
Debiche	D6F61	M	3547575.1	717067.1	173.5	26/01/2013	2.22	23.9	7.74	1.78	14.2	8.41	12.6	0.66	5.38	4.43	
Rouissat III	D3F10	S	3535068.1	722352.1	248	1996	3.1	26.1	7.27	2.38	14.27	6.89	13.05	0.4	3.36	5.42	
Said Otba I	D2F71	S	3557412.4	718272.8	211.9	26/01/2013	5.63	25.1	7.34	2.38	14.3	6.86	13.1	0.4	3.36	5.43	
Rouissat III	D3F10	S	3535068.1	722352.1	248	20/01/2013	2.32	18.9	7.98	1.65	15.2	8.64	12.6	1.56	5.79	4.25	
Ifri	D1F151	S	3538891.7	721060.5	204	27/01/2013	2.37	22.9	7.79	1.75	15.4	8.31	13.7	0.22	5.17	4.75	
Said Otba	D2F66	S	3540257.3	720085.4	216	31/01/2013	2.38	24.9	7.91	2.19	16.1	8.65	16.5	0.74	4.93	4.29	
Oglat Larbaâ	D6F64	M	3566501.4	729369.3	177	31/01/2013	2.43	23.7	7.62	2.3	16.3	8.65	13.6	0.71	5.86	4.97	
SAR Mekhadma	D1F91	S	3536757.7	717822.3	221	03/02/2013	2.47	25.8	7.75	3.43	16.5	8.53	16.1	0.68	5.27	4.92	
Sidi Kouiled	D9F12	S	3540855.1	729055.4	329	24/01/2013	2.57	21.3	8.05	4.65	16.8	8.85	16.1	0.79	6.21	5.01	
Ain N'sara	D6F50	S	3559323.6	716868.4	255	25/01/2013	3.36	25.7	7.36	1.98	16.9	9.71	15.9	0.35	3.39	7.87	
A.Louise	D4F73	S	3573523.4	721904.6	310	26/01/2013	2.57	24	7.49	1.98	17.4	9.04	13.9	1.99	5.78	5.05	
Ghazalet A.H	D6F79	M	3587502.0	720356.8	119	02/02/2013	2.84	22.5	7.55	3.47	17.4	9.93	16.6	0.62	6.24	4.96	
Ain moussa II	D9F30	S	3573814.1	719665.1	220.6	02/02/2013	7.52	23.9	7.52	2.37	17.5	8.24	17.3	0.39	3.1	6.46	
Ain N'sara	D6F50	S	3559323.6	716868.4	255	02/02/2013	2.62	23.8	7.65	2.11	17.7	9.19	15.5	1.13	6.11	4.73	
H.Milioud	D1F135	M	3547557.1	717067.1	173	03/02/2013	2.76	21.6	7.55	3.32	17.9	9.22	16.5	1.01	6.17	4.91	
El Bour	D6F97	S	3540936.5	715816.0	169	25/01/2013	2.65	19.9	8.02	2.14	17.9	9.28	15.8	1.6	5.84	4.73	
H.Milioud	D1F135	M	3547557.1	717067.1	173	1996	2.07	22.7	8.1	2.8	18.08	5.73	16.61	0.51	3.65	4.26	
N'goussa El Hou	D6F51	S	3556256.7	718979.5	198	31/01/2013	2.97	22.9	7.52	2.03	18.4	9.63	17.1	0.45	6.17	4.99	
El Koum	D6F67	S	3573694.1	721639.7	143	21/01/2013	3.07	22.9	8.09	3.52	18.4	9.71	17.9	0.32	6.49	5.14	
El Koum	D6F67	S	3573694.1	721639.7	143	1996	2.5	25	7.6	1.5	18.79	7.17	10.18	3.43	4.97	5.81	
ITAS	D1F150	M	3536186.6	717046.1	93.1	21/01/2013	3.66	23.9	7.54	1.48	18.8	7.07	10.1	3.41	4.94	5.77	
Ain moussa V	D9F13	M	3538409.2	718680.2	210.2	08/02/2013	2.39	25.3	7.22	2.28	19.4	9.45	18.8	0.39	3.31	7.61	
El Bour	D4F94	M	3536245.2	722641.7	100.6	1996	2.3	21.2	7.9	1.58	20.05	7.21	12.09	2.62	5.76	5.17	
Rouissat I	D3F18	M	3535564.2	722498.9	80.4	26/01/2013	3.13	23	8.1	3.15	21.2	11.1	19.6	0.87	7.08	6.01	
Rouissat I	D3F18	M	3535564.2	722498.9	80.4	1996	2	20	7.84	1.86	21.66	8.46	17.72	1.19	5.05	6	
St. pompage chott	D5F80	S	3541656.9	723521.9	224.1	04/02/2013	3.28	24.5	8.23	3.91	22.1	11.9	19.9	2.13	7.64	6.28	
Chott Palmeraie	D5F77	S	3538219.3	725541.3	242.8	05/02/2013	3.37	24.6	7.53	3.26	22.3	12.1	20.9	1.15	8.25	5.78	
Bour El Haicha	D1F134	M	3545533.1	720391.7	86	05/02/2013	3.4	22.2	7.34	4.13	23.2	12.2	21.2	1.49	8.61	6.01	
Abazat	D2F69	M	3552504.9	717286.3	137.1	03/02/2013	3.54	24.6	7.61	2.24	24.7	12.7	21.1	1.65	8.45	6.47	
Garet Chemia	D1F113	S	3536174.1	716808.5	213.7	28/01/2013	4.05	28	7.3	2.21	25.9	9.47	25.4	0.57	3.64	7.17	
Frane	D6F62	M	3570175.8	717133.8	167.5	27/01/2013	3.79	24.2	7.95	2.27	25.9	13.5	22.6	0.64	8.91	7.16	
Oum Raneb	D6 F69	M	3540451.1	721919.8	215.8	25/01/2013	4.2	24.1	7.03	2.61	27.9	8.67	22.9	0.62	4.42	7.96	
N'goussa El Hou	D6F51	S	3556256.7	718979.5	198	1996	3.15	23.2	8	2.58	28.39	8.61	23.14	0.62	4.46	8.01	
H.Milioud Benyaza	D1F138	M	3551192.5	717042.1	88.9	28/01/2013	3.85	25.2	7.61	2.44	28.4	14.2	23.9	1.66	10.01	7.12	
Ain Laarab	D6F49	M	3558822.6	716799.1	156.5	28/01/2013	3.97	23.7	7.33	2.16	28.9	9.01	23.9	0.53	5	7.72	
H.Milioud Benyaza	D1F138	M	3551192.5	717042.1	88.9	1996	2.9	22.8	7.5	2.16	28.92	9.03	23.87	0.52	4.99	7.7	
Rouissat	D3F8	M	3545470.7	732837.6	332.4	03/02/2013	4.38	25.4	7.51	1.71	29.8	8.33	22.8	1.23	6.23	6.08	
Rouissat	D3F8	M	3545470.7	732837.6	332.4	1996	6.16	25.3	7.22	1.71	29.81	8.33	22.86	1.23	6.23	6.08	
Ain El Arch	D3F26	M	3534843.9	723831.8	93.6	1996	5.11	25.1	7.45	1.56	34.68	8.94	23.98	0.87	8.38	6.5	
St. pompage chott	D5F80	S	3541656.9	723521.9	224.1	1996	3.69	25.4	7.67	2.28	42.22	13.53	36.77	1.12	7.43	9.73	

M = Mio-pliocene aquifer; S = Senonian aquifer.

Chemical and  
isotopic data from  
groundwaters in  
Sahara

R. Slimani et al.

Title Page

Abstract

Conclusions

Tables

Figures

◀

▶

Back

Close

Full Screen / Esc

Printer-friendly Version

Interactive Discussion



**Table 3.** Field and analytical data for the Phreatic aquifer.

Locality	Site	Lat.	Long.	Elev.	Date	EC	<i>t</i>	pH	Alk.	Cl <sup>-</sup>	SO <sub>4</sub> <sup>2-</sup>	Na <sup>+</sup>	K <sup>+</sup>	Mg <sup>2+</sup>	Ca <sup>2+</sup>	Br <sup>-</sup>
		/m				mS cm <sup>-1</sup>	°C					mmol L <sup>-1</sup>				
Khezana	P433	3597046	719626	118	20/01/2013	2.09	22.7	9.18	1.56	12.02	7.3	13	0.99	4.34	2.8	
Khezana	P433	3597046	719626	118	1996	2	22.1	8.86	1.46	12	6.87	11.57	0.93	4.4	2.9	
Hassi Miloud	P059	3547216	718358	124	27/01/2013	2.1	23.9	8.15	1.86	13	7.3	12.6	1.25	4.43	3.43	0.024
Ain Kheir	PL06				1996	4.01	23.79	7.52	1.86	14.15	17.89	15.89	0.61	10.61	7.5	
Hassi Naga	PLX3	3584761.4	717604.5	125	20/01/2013	2.93	23	8.09	2.04	17.7	9.4	16.6	0.93	5.75	5	0.031
	LTP 30				1996	4.08	23.73	7.12	5.25	18.21	9.97	24.29	0.41	1.43	8.13	
Maison de culture	PL31	3537988	720114	124	1996	2.51	23.83	8.08	1.46	18.91	7.8	26.05	0.62	2.13	2.99	
El Bour	P006	3564272	719421	161	1996	2.96	23.43	7.88	1.27	18.99	7.74	12.41	2.69	5.32	5.31	
Hassi Miloud	P059	3547216	718358	124	1996	2.77	23.45	7.83	2.27	20.83	9.366	34.17	4.25	1.35	0.86	
Oglet Larbaa	P430	3567287.5	730058.8	139	24/01/2013	4.5	27.5	8.29	3.29	22.1	12.4	21.8	2.59	8.61	5.47	
Maison de culture	PL31	3537988	720114	124	28/01/2013	3.7	22.2	8.23	4.22	22.6	8.6	28.4	2.21	4.01	3.17	
France El Koum	P401	3572820.2	719721.4	112	20/01/2013	3.44	27.5	7.52	2.21	23.3	13.4	21.8	1.86	8.25	6.28	0.032
Gherbouz	PL15	3537962	718744	134	1996	2.47	23.47	7.72	2.99	23.54	13.97	50.56	2.82	0.98	0.25	
Bour El Haicha	P408	3544999.3	719930.6	110	1996	2.43	23.46	7.75	2.39	24.16	13.23	41.89	6.08	2.34	0.84	
Station d'épuration	PL30	3538398	721404	130	1996	5.51	23.80	7.39	3.01	24.32	21.22	24.26	0.88	20.16	2.23	
France Ank Djemel	P422	3575339	718875	109	20/01/2013	4.08	24.2	8.38	4.39	25.3	9.5	23.7	1.77	4.18	7.91	0.025
Route Ain Bida	PLX2	3537323.9	724063.3	127	1996	4.7	23.61	7.22	2.02	25.68	10.36	14.83	0.24	9.33	7.36	
H Chegga	PLX4	3577944.8	714428.5	111	20/01/2013	4.1	25.2	7.61	3.03	26.2	9.8	24	2.32	4.96	7.46	0.033
Hassi Miloud	P058	3547329.7	716520.7	129	27/01/2013	3.66	24.6	8.1	3	27.7	10.6	19	2.29	9.09	6.55	
Route Ain Moussa	P057	3548943	717353	133	1996	5.3	23.44	7.69	1.34	28.21	11.48	17.58	2.03	11.48	5.8	
Route El Goléa	P115	3533586	714060	141.6	1996	2.62	23.68	7.65	2.84	28.77	14.52	58.74	0.03	0.83	0.73	
Mekmehad	PL05	3537109.4	718419.1	137	1996	23.87	7.76	1.75	30.87	16.66	24.9	0.97	15.69	4.49		
Polyclinique Belabès	PL18	3537270	721119	119	31/01/2013	4.67	22.2	7.89	1.78	31.2	15.4	21.3	3.87	11.17	8.37	
H Chegga	PLX4	3577944.8	714428.5	111	1996	4.49	23.67	7.58	1.5	31.52	10.08	20.05	5.87	7.53	6.5	
Route El Goléa	P116	3532463	713715	117	1996	5.62	23.69	7.62	1.45	31.94	12.83	22.23	0.8	10.55	7.89	
Gherbouz	PL15	3537962	718744	134	21/01/2013	4.65	23.3	8.16	1.78	32.4	14.6	27.8	0.8	6.76	10.83	
Route El Goléa	P117	3531435	713298	111	1996	4.77	23.70	7.70	1.55	32.81	12.85	30.18	0.96	9.19	5.74	
Route Ain Moussa	P057	3548943	717353	133	26/01/2013	5.7	26.2	7.64	2.48	33.5	11.9	27.7	5.93	5.98	7.57	
Ecole paramédicale	PL32	3538478	720170	131	21/01/2013	5.72	22.9	8.21	1.96	33.6	12.1	29.2	3.35	6.36	8.17	
DSA	PL10	3537055	719746	114	1996	6.08	23.71	7.69	1.32	35.01	13.52	8.6	1.92	19.37	7.23	
Route El Goléa	P117	3531435	713298	111	03/02/2013	5.5	25	7.72	3.25	35.4	13.8	37.1	3.04	8.45	5.68	
Route El Goléa	P116	3532463	713715	117	03/02/2013	5.8	22.5	8.04	1.66	36.3	11.6	28.5	3.21	6.75	8.37	
Station d'épuration	PL30	3538398	721404	130	31/01/2013	5.29	25.1	7.84	4.1	38.4	14.6	28.5	4.45	11.62	8.14	
Hassi Debich	P416	3581097	730922	106	24/01/2013	5.5	23.7	8.86	0.35	38.6	18	22.3	0.89	4.8	21.26	
DSA	PL10	3537055	719746	114	28/01/2013	5.51	24.6	8.44	2.37	38.8	16.9	36.9	1.93	9.03	9.21	
Hôpital	LTPSN2	3538292.9	720442.9	132	27/01/2013	6.09	25.4	7.78	1.62	39.7	11.7	36	8.43	5.11	5.97	
PARC SONACOM	PL28	3536077	719558	134	21/01/2013	6.08	24.5	8.13	1.82	39.8	11.8	30.6	5.2	7.14	8.46	
Bour El Haicha	P408	3544999.3	719930.6	110	27/01/2013	6.22	23.1	8.07	1.82	42	19.1	27.5	13.21	13.39	8.12	
Route Ain Moussa	P056	3549933	717022	128	1996	7.62	23.65	7.93	0.56	42.14	10.72	18.87	1.86	12.63	9.32	
Route Ain Moussa	P056	3549933	717022	128	26/01/2013	5.98	24.6	7.63	2.16	42.5	17.9	32.1	8.03	12.49	8.07	
Ecole Okba B. Nafaa	PL41	3538660	719831	127	31/01/2013	6.26	24.1	7.68	2.11	44.9	13.2	36.2	11.8	6.32	6.68	

Chemical and  
isotopic data from  
groundwaters in  
Saara

R. Slimani et al.

Title Page

Abstract

Conclusions

Tables

Introduction

References

Figures

◀

▶

Back

Close

Full Screen / Esc

Printer-friendly Version

Interactive Discussion



# Chemical and isotopic data from groundwaters in Sahara

R. Slimani et al.

Locality	Site	Lat.	Long.	Elev.	Date	EC	t	pH	Alk.	Cl-	SO <sub>4</sub> <sup>2-</sup>	Na <sup>+</sup>	K <sup>+</sup>	Mg <sup>2+</sup>	Ca <sup>2+</sup>
		m				mS cm <sup>-1</sup>	°C			mmol L <sup>-1</sup>					
PARC HYDRAULIQUE	P419	3539494	725605	132	31/01/2013	7.03	26.4	7.84	2.05	45.1	14.4	41.4	10.78	5.95	6.91
Parc hydraulique	PL13	3536550	720200	123	21/01/2013	7.22	24.5	7.51	3.24	47.8	14.5	44.4	10.55	6.35	6.59
Mekhdama	PL25	3536230	718708	129	21/01/2013	7.64	27.1	7.94	1.78	48	14.5	42.9	6.56	7.4	7.61
Said Olba	P506	3535528.1	725075.1	126	04/02/2013	8.32	24.3	8.12	1.71	52.6	14.6	42.8	10.97	7.51	7.83
Said Olba	P506	3535528.1	725075.1	126	1996	6.7	23.28	7.46	1.8	54.39	17.58	33.32	4.11	22.16	5.17
Mekhdama	P566	3540433.1	719661.3	115	27/01/2013	9	24.6	7.64	1.72	62.5	15.2	71.6	3.03	4.61	6.06
Mekhdama	PL17	3536908	718511	130	21/01/2013	9.4	24.5	8.06	3.39	63.2	15.6	77.2	2.51	4.08	5.11
Palm. Gar Krima	P413	3530116.2	722775.1	130	04/02/2013	10.09	30.2	7.91	1.63	63.6	21.5	88.3	4.08	2.41	4.65
Mekhdama	PL25	3536230	718708	129	1996	9.5	23.72	7.96	0.63	75.57	10.62	10.22	2.64	32.94	9.54
Said Olba (Bab sbaa)	P066	3542636.5	719857.4	126	1996	7.75	23.48	7.62	1.51	80.23	12.45	45.87	2.46	23.59	5.91
CEM Malek B. Nabi	PL03	3540010.9	725738.1	130	1996	7.34	23.86	7.60	3.04	84.14	30.58	108.55	2.23	10.17	8.99
ENTV	PL21	3536074	721268	128	1996	9.73	23.82	7.25	4.46	84.26	23.68	61.62	3.75	33.53	1.88
Hôtel Transat	PL23	3538419	720950	126	28/01/2013	15	24.2	8.2	4.53	86.6	16.7	79.9	3.21	14.54	6.85
ENTV	PL21	3536074	721268	128	28/01/2013	16.41	25.7	7.45	1.97	99.9	17.4	85.5	5.7	15.66	7.6
Mekhdahad	PL05	3537109.4	718419.1	137	21/01/2013	16.8	24.8	7.64	2.02	101.3	17.7	85.9	5.85	16.69	7.59
Beni Thour	PL44	3536039.3	721673.9	134	1996	4.68	23.85	7.19	2.74	109.75	67.21	134.67	5.71	42.02	8.77
Tazegart	PLSN1	3537675	719416	125	22/01/2013	17.08	24.9	8	3.41	114.2	18.1	92.9	12.8	16.85	7.81
CEM Malek B. Nabi	PL03	3540010.9	725738.1	130	27/01/2013	10.84	23.1	7.54	3.29	117.3	14.7	116.4	2.06	8.99	7.24
El Bour	P006	3564272	719421	161	03/02/2013	18.31	23.6	7.76	6.26	131.9	18.1	96.3	8.61	27.11	7.99
Ain Moussa	P015	3551711	720591	103	1996	12.42	23.62	7.71	2.38	134.68	28.2	72.98	3.1	52.44	6.25
Station de pompage	PL04	3541410.1	723501.1	138	27/01/2013	19.01	26.4	7.85	4.03	138	16.7	108.8	13.06	19.51	8.72
Drain Chott Ouardla	D.Ch				1996	23.88	7.67	2.68	142.22	24.5	96.31	3.16	44.22	3.02	
Beni Thour	PL44	3536039.3	721673.9	134	28/01/2013	20.18	25.8	7.8	4.96	153	17.7	125.9	6.29	22.83	8.08
CNCM	PL27	3535474	718407	126	21/01/2013	21.23	24.8	8.11	1.7	169.4	18.4	130.3	4.89	27.81	8.63
Bamendil	P076	3540137	716721	118	26/01/2013	22.31	27.2	7.57	4.33	171.5	17.1	130.8	6.32	28.01	8.83
N'Goussa	P041	3559563	716543	135	26/01/2013	25.94	24.5	8.18	7.95	208.6	13.4	198.9	3.61	11.81	8.75
N'Goussa	P009	3559388	717707	123	26/01/2013	27.51	28.4	8.39	11.45	208.8	15.8	195.1	2.65	18.7	9.01
LTP16					1996	23.88	7.67	2.68	142.22	24.5	96.31	3.16	44.22	3.02	
P100					1996	11.53	23.78	7.48	3.84	213.35	48.63	147.9	7.46	75.31	4.25
Chott Adjadja Aven	PLX1	3540758.8	726115.6	132	28/01/2013	32.93	23.4	7.95	4.44	245.6	20.9	141.4	26.88	44.56	17.66
Route Frane	P003	3569043	721496	134	02/02/2013	31.03	23.5	8.01	6.91	252.7	17.9	208.2	9.41	29.99	10.03
El Bour-N'gouca	P007	3562236	718651	129	26/01/2013	30.07	28.4	7.76	5.42	254.7	15.5	209.2	10.43	28.82	7.51
Route Ain Bida	PLX2	3537323.9	724063.3	127	21/01/2013	43.25	25.7	8.07	5.15	262.2	93	270.4	15.5	62.77	21.46
Ain Moussa	P015	3551711	720591	103	25/01/2013	32.02	22.7	8.03	2.95	263	15.4	206.9	6.56	32.12	9.95
Ain Moussa	P402	3549503	721514	138	25/01/2013	60	28.7	8.6	7.69	313.2	93.9	442.8	23.26	12.56	10.17
Route Frane	P001	3572148	722366	127	1996	23.63	8.37	4	323.62	58.13	331.43	5.01	49.77	3.97	
Ain Moussa	P014	3551466	719339	131	1996	23.40	7.31	3.98	336.96	64.29	328.67	5.53	62.37	5.45	
N'Goussa	P019	3562960	717719	113	02/02/2013	60.58	27.8	7.65	6.02	356.2	96	432.5	29.77	21.02	26.23
N'Goussa	P018	3562122	716590	110	26/01/2013	61.06	26.2	8.42	6.46	372.4	8.23	347.1	22.64	60.71	26.63
Ain Moussa	P014	3551466	719339	131	25/01/2013	49.04	25.2	7.89	1.8	399.7	21.1	389.3	2.41	18.97	7.39
Route Sedrata	P113	3535858	714576	105	03/02/2013	62.24	24.8	8.2	5.96	414.8	83.8	362.7	33.34	70.23	26.51
N'Goussa	P009	3559388	717707	123	1996	23.27	7.84	2.4	426.85	57.81	393.83	9.13	59.13	12.02	



**Table 5.** Field and analytical data for the Phreatic aquifer (continued).

Locality	Site	Lat.	Long.	Elev.	Date	EC mS cm <sup>-1</sup>	t °C	pH	Alk.	Cl <sup>-</sup>	SO <sub>4</sub> <sup>2-</sup> mmol L <sup>-1</sup>	Na <sup>+</sup>	K <sup>+</sup>	Mg <sup>2+</sup>	Ca <sup>2+</sup>
Route Frane	P001	3572148	722366	127	02/02/2013	66.16	28.3	7.24	6.49	468.7	101.5	350.3	25.96	116.21	35.31
Sekhbet Sifioune	P031	3577804	720172	120	1996		23.75	7.31	6.32	481.83	43.35	326.82	12.61	94.15	23.56
Sekhbet Sifioune	P031	3577804	720172	120	02/02/2013	75.96	27.9	8.06	5.85	500.3	110.3	470.5	28.67	79.12	35.47
Route Frane	P002	3570523	722028	108	1996		23.81	7.76	6.29	522.39	182.95	653.78	9.97	104.7	10.99
Sekhbet Sifioune	P030	3577253	721936	130	1996		23.52	7.72	4.43	527.7	123.48	533.79	11.59	106.21	10.65
Oum Raneb	P012	3554089	718612	114	25/01/2013	64.05	30.3	7.83	7.77	534.3	20.9	529.6	6.41	19.73	4.73
Oum Raneb	P012	3554089	718612	114	1996		23.41	7.46	2.72	539.35	60.64	413.55	5.55	112.77	9.42
ANK Djemel	P423	3540881	723178	102	31/01/2013	90.8	23.5	7.48	6.19	636.5	101.3	495.5	38.31	125.81	30.32
Said Otba-Chott	P096	3540265	724729	111	1996		23.59	7.71	3.69	645.07	78.46	357.28	5.89	208.4	12.86
Sekhbet Sifioune	P030	3577253	721936	130	03/02/2013	64.66	23.1	7.83	3.71	671.8	90.3	742.9	15.97	41.46	7.65
N'Goussa	P017	3560256	715781	130	26/01/2013	100.1	31	7.13	3.78	679.3	114.1	597.8	10.71	125.85	26.29
ANK Djemel	P021	3573943	723161	105	1996		23.55	7.43	4.24	700.77	154.45	605.68	53.6	163.08	14.24
Station de pompage	PL04	3541410.1	723501.1	138	1996		23.57	7.42	2.37	716.27	34.75	560.07	7.04	99.58	11.04
Route Frane	P002	3570523	722028	108	02/02/2013	62.82	26.9	7.57	1.65	748.5	62.6	651.15	14.72	77.72	27.29
Said Otba-Chott	P096	3540265	724729	111	03/02/2013	68.31	25.9	8.7	1.24	771	53.1	615.9	23.46	69.64	50.39
N'Goussa	P19	3562960	717719	113	1996		23.30	7.72	2.42	779.13	77.13	711.46	9.23	95.59	12.05
Said Otba(Bab sbaa)	P066	3542636.5	718957.4	126	03/02/2013	150.6	26.2	7.18	12.29	799.1	283	1249.7	18.95	37.63	18.06
ANK Djemel	P021	3573943	723161	105	24/01/2013	82.28	29.6	7.64	2.35	800.4	94.4	824	10.99	53.35	25.39
N'Goussa	P018	3562122	716590	110	1996		23.29	7.46	1.24	816.87	81	244.21	49.54	319.35	24.76
Oum Raneb	P162	3546133	725129	98	25/01/2013	160	30.7	7.15	2.43	842.8	289.9	1309.9	13.3	33.47	17.74
Route Sedrata	P113	3535586	714576	105	1996		23.66	7.70	2.81	954.89	124.85	997.52	13.3	86.69	11.67
Oum Raneb	P212	3547234	722931	110	05/02/2013	114.9	27.4	7.44	2.88	980.1	15.5	930.8	7.53	23.19	14.24
Hôtel Transat	PL23	3538419	720950	126	1996		23.49	7.37	3	1103.31	94.49	707.81	19.14	270.91	13.3
Sekhbet Sifioune	P023	3577198	725726	99	1996		23.32	7.42	2.25	1176.99	91.14	1058.21	11.72	133.47	12.41
Sekhbet Sifioune	P034	3579698	725633	97	05/02/2013	130	34.9	8.08	1.76	1189.1	14.7	1055.1	18.27	56.37	17.38
Sekhbet Sifioune	P023	3577198	725726	99	05/02/2013	117.9	29.4	8.19	1.85	1209.3	15.6	1129.4	8.38	42.85	10.15
Chott Adjadja	PLX1	3540758.8	726115.6	132	1996		23.60	8.02	3.82	1296.65	134.01	1458.73	5.24	47.98	4.34
Sekhbet Sifioune	P063	3545586.8	725667.4	99	1996		23.50	7.46	1.94	1379.35	139.61	1257.42	18.6	182.26	10.03
LTP06					1996		23.77	7.64	7.84	1636.86	712.09	2621.61	41.55	190.51	13.34
Bamendil	P076	3540137	716721	118	1996		23.53	7.71	5.72	1743.55	143.36	1321.87	26.85	331.38	12.26
El Bour-N'gouca	P007	3562236	718651	129	1996		23.26	7.67	1.41	1860.53	91.55	1434.73	26.2	278.77	13.25
Sekhbet Sifioune	P063	3545586.8	725667.4	99	05/02/2013	178.9	26.7	7.67	1.43	1887.9	92.9	1455.8	26.66	282.88	13.44
					1996		23.39	7.79	4.53	2106.07	18.27	1765.47	27.33	171.23	6.54
					1996		23.58	7.49	1.49	2198.58	182.08	1957.53	29.49	278.18	10.44
					1996		23.42	7.59	1.1	2330.85	101.22	1963.71	52.19	248.1	11.24
					1996		23.51	7.54	3.35	2335.67	222.08	2302.25	26.84	219.9	7.19
Oum Raneb	PZ12	3547234	722931	110	1996		23.31	7.59	2.21	2405.55	109.92	2178.55	25.23	199.35	12.65
Hassi Debich	P416	3581097	730922	106	1996		23.33	7.84	4.33	2433.73	178.87	2361.09	24.34	196.07	9.2
N'Goussa	P041	3559563	716543	135	1996		23.38	7.94	2.13	2599.74	324.58	2878.99	44.57	152.83	10.97
Sekhbet Sifioune	P034	3579698	725633	97	1996		23.34	7.85	1.95	2752	134.14	2616.77	24.42	180.14	10.48
					1996		23.37	6.87	1.94	4189.51	201.44	4042.62	17.9	257.81	9.23
Sekhbet Sifioune	P074				1996		23.54	6.47	4.17	4356.48	180.88	2759.9	57.4	930.06	22.63
Sekhbet Sifioune	P037				1996		23.36	6.92	1.95	4583.84	261.06	24.42	3.74	347.57	7.86
Sekhbet Sifioune	P036				1996		23.35	7.54	1.4	4972.75	108.12	4692.23	36.84	221.13	9.63



**Table 6.** Isotopic data  $^{18}\text{O}$  and  $^3\text{H}$  and chloride concentration in Continental Intercalaire, Complexe Terminal and Phreatic aquifers.

Phreatic aquifer											
Piezometer	$\text{Cl}^-$ mmol L <sup>-1</sup>	$\delta^{18}\text{O}$ ‰	$^3\text{H}$ UT	Piezometer	$\text{Cl}^-$ mmol L <sup>-1</sup>	$\delta^{18}\text{O}$ ‰	$^3\text{H}$ UT	Piezometer	$\text{Cl}^-$ mmol L <sup>-1</sup>	$\delta^{18}\text{O}$ ‰	$^3\text{H}$ UT
P007	1860.5	-2.49	0	PL15	23.54	-7.85	0.6(1)	P074	4356.4	3.42	6.8(8)
P009	426.85	-6.6	1.2(3)	P066	80.23	-8.14	0.8(1)	PL06	14.15	-8.13	1.0(2)
P506	54.39	-6.83	1.6(3)	PL23	1103.32	-6.1	0	PL30	24.32	-7.48	2.4(4)
P018	818.67	-2.95	6.2(11)	P063	1379.3	-3.4	8.7(15)	P002	522.39	-5.71	0.6(1)
P019	779.13	-4.67	5.6(9)	P068	2335.6	-3.04	8.8(14)	PL21	84.26	-7.65	1.2(2)
PZ12	2405.5	-2.31	8.1(13)	P030	527.7	-6.57	2.4(4)	PL31	18.91	-7.38	1.6(3)
P023	1176.9	-2.62	0.2(1)	P076	1743.5	-5.56	2.8(5)	P433	12	-8.84	0
P416	2433.7	-7.88	5.9(9)	P021	700.7	-5.16	2.6(4)	PL03	84.14	-7.35	1.7(3)
P034	2752	-1.77	5.7(9)	PL04	716.27	-2.89		PL44	109.75	-8.82	1.0(2)
P036	4972.7	3.33	2.1(4)	P093	2198.5	-2.64	5.1(8)	PL05	30.87	-7.44	1.9(3)
P037	4953.8	3.12	1.8(3)	P096	645.07	-6.13	4.8(8)	P408	24.16	-7.92	0
P039	4189.5	0.97	2.2(4)	PLX1	1296.6	-5.6	1.1(2)	P116	31.94	-7.18	1.1(2)
P041	2599.7	-0.58	7.3(13)	PLX2	25.68	-7.6	1.3(2)	LTP 16	213.35	-7.48	1.6(3)
P044	2106.1	-4.46	2.7(5)	P015	134.68	-6.77	3.0(5)	P117	32.81	-6.92	0.1
P014	336.96	-6.9	2.8(5)	P001	323.62	-4.66	2.5(4)	PL10	35.01	-7.31	0.2(1)
P012	539.3	-6.41	2.2(4)	P100	235.01	-5.81	0	PL25	75.57	-7.41	0.9(2)
P042	2330.8	2.05	6.0(10)	P056	42.14	-7.03	2.9(5)	LTP30	18.21	-7.5	1.1(2)
P006	18.98	-6.64	0.5(1)	P113	954.89	-4.75	0.8(2)	LTP06	1638.6	-1.97	2.8(5)
P057	28.21	-7.33	1.1(2)	PLX4	31.52	-7.1	0.3(1)	P031	481.83	-6.06	3.0(5)
P059	20.83	-7.81	0	P115	28.77	-2.54	6.8(12)				
Complexe Terminal aquifer											
Borehole	$\text{Cl}^-$ mmol L <sup>-1</sup>	$\delta^{18}\text{O}$ ‰	$^3\text{H}$ UT	Borehole	$\text{Cl}^-$ mmol L <sup>-1</sup>	$\delta^{18}\text{O}$ ‰	$^3\text{H}$ UT	Borehole	$\text{Cl}^-$ mmol L <sup>-1</sup>	$\delta^{18}\text{O}$ ‰	$^3\text{H}$ UT
D5F80	42.22	-7.85		D1F138	28.92	-8.13	0.7(1)	D2F71	13.53	-8.23	0.6(1)
D3F8	29.81	-8.14	1.4(2)	D3F18	21.66	-8.23	0.2(1)	D7F4	10.6	-8.27	0.1(1)
D3F26	34.68	-7.97	0.8(1)	D3F10	14.27	-7.88	1.5(2)	D2F66	11.02	-8.3	
D4F94	20.05	-8.18	0.6(1)	D6F51	28.39	-7.9	0.7(1)	D1F151	10.75	-8.32	0.4(1)
D6F67	18.79	-8.23	3.7(6)	D1F135	18.08	-7.97	1.1(2)	D6F64	11.36	-8.28	4.3(7)
Continental Intercalaire aquifer											
Borehole	$\text{Cl}^-$ mmol L <sup>-1</sup>	$\delta^{18}\text{O}$ ‰	$^3\text{H}$ UT	Borehole	$\text{Cl}^-$ mmol L <sup>-1</sup>	$\delta^{18}\text{O}$ ‰	$^3\text{H}$ UT	Borehole	$\text{Cl}^-$ mmol L <sup>-1</sup>	$\delta^{18}\text{O}$ ‰	$^3\text{H}$ UT
Hadeb I	5.8	-8.02	0	Hadeb II	6.19	-7.93	0.1(1)	Aouinet Moussa	6.49	-7.88	1.1(2)

## Chemical and isotopic data from groundwaters in Sahara

R. Slimani et al.

Title Page

Abstract

Introduction

Conclusions

References

Tables

Figures

◀

▶

◀

▶

Back

Close

Full Screen / Esc

Printer-friendly Version

Interactive Discussion



## Chemical and isotopic data from groundwaters in Sahara

R. Slimani et al.

[Title Page](#)

[Abstract](#)

[Introduction](#)

[Conclusions](#)

[References](#)

[Tables](#)

[Figures](#)

[◀](#)

[▶](#)

[◀](#)

[▶](#)

[Back](#)

[Close](#)

[Full Screen / Esc](#)

[Printer-friendly Version](#)

[Interactive Discussion](#)



## Chemical and isotopic data from groundwaters in Sahara

R. Slimani et al.

[Title Page](#)

[Abstract](#)

[Introduction](#)

[Conclusions](#)

[References](#)

[Tables](#)

[Figures](#)

[◀](#)

[▶](#)

[◀](#)

[▶](#)

[Back](#)

[Close](#)

[Full Screen / Esc](#)

[Printer-friendly Version](#)

[Interactive Discussion](#)



**Table 8.** Summary of mass transfer for geochemical inverse modeling. Phases and thermodynamic database are from Phreeqc 3.0 (Parkhurst and Appelo, 2013).

Phases	Stoichiometry	Cl/CT	CT/Phrl I	Rainwater/P036	Phrl/Phrl II 60%/40 %
Calcite	CaCO <sub>3</sub>	–	–6.62E-06	–1.88E-01	–2.26E-01
CO <sub>2</sub> (g)	CO <sub>2</sub>	–6.88E-05	–	8.42E-04	5.77E-04
Gypsum	CaSO <sub>4</sub> .2H <sub>2</sub> O	4.33E-03	–	1.55E-01	1.67E-01
Halite	NaCl	7.05E-03	3.76E-03	6.72E+00	1.28E+00
Sylvite	KCl	2.18E-03	1.08E-03	4.02E-01	–
Bloedite	Na <sub>2</sub> Mg(SO <sub>4</sub> ) <sub>2</sub> .4H <sub>2</sub> O	–	1.44E-03	–	–
Huntite	CaMg <sub>3</sub> (CO <sub>3</sub> ) <sub>4</sub>	–	–	4.74E-02	5.65E-02
Ca ion exchange	CaX <sub>2</sub>	–1.11E-03	–	–	–
Mg ion exchange	MgX <sub>2</sub>	1.96E-03	–	1.75E-01	–2.02E-01
Na ion exchange	NaX	–	–	–	3.92E-01
K ion exchange	KX	–1.69E-03	–	–3.49E-01	1.20E-02

Values are in mol kg<sup>-1</sup> H<sub>2</sub>O. Positive (mass entering solution) and negative (mass leaving solution) phase mole transfers indicate dissolution and precipitation, respectively; – indicates no mass transfer.

# Chemical and isotopic data from groundwaters in Sahara

R. Slimani et al.

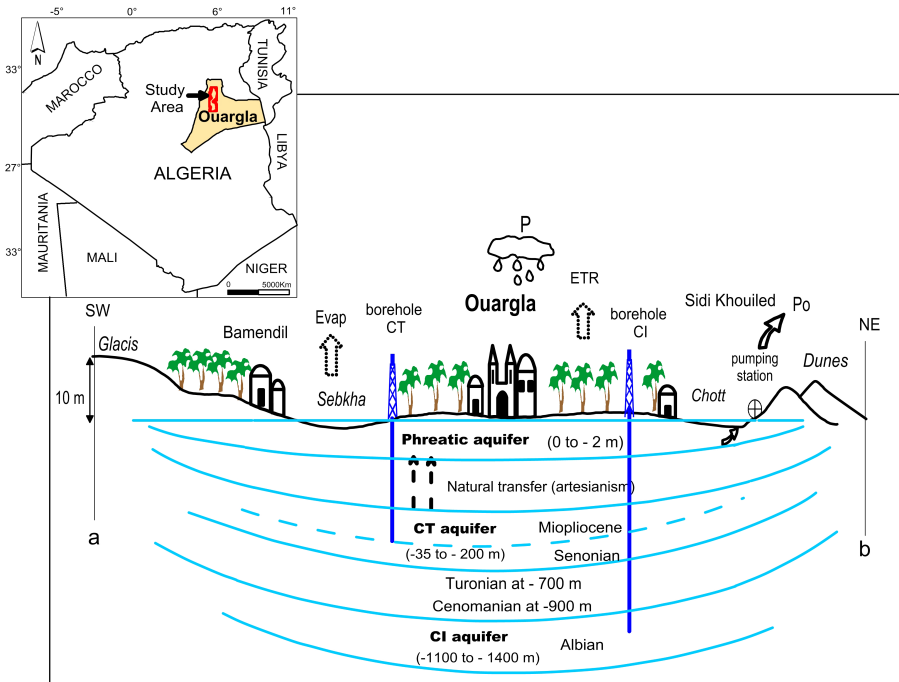


**Figure 1.** Localisation and schematic relations of aquifers in Ouargla. Blue lines represent limits between aquifers, and the names of aquifers are given in bold letters; as the limit between Senonian and Miopliocene aquifers is not well defined, a dashed blue line is used. Names of villages and cities are given in roman (Bamendil, Ouargla, Sidi Khouiled), while geological/geomorphological features are in italic (Glacis, Sebkha, Chott, Dunes). Depths are relative to the ground surface. Letters a and b refer to the cross section (Fig. 2) and to the localisation map (Fig. 3).

# Chemical and isotopic data from groundwaters in Sahara

R. Slimani et al.

Title Page

## Abstract

Introduction

## Conclusion

## References

## Tables

## Figures

## Tables

## Figures

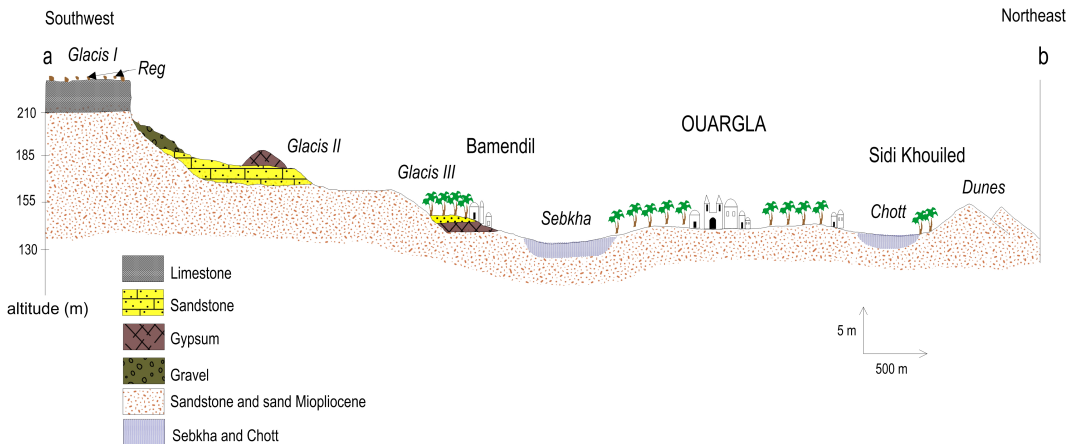
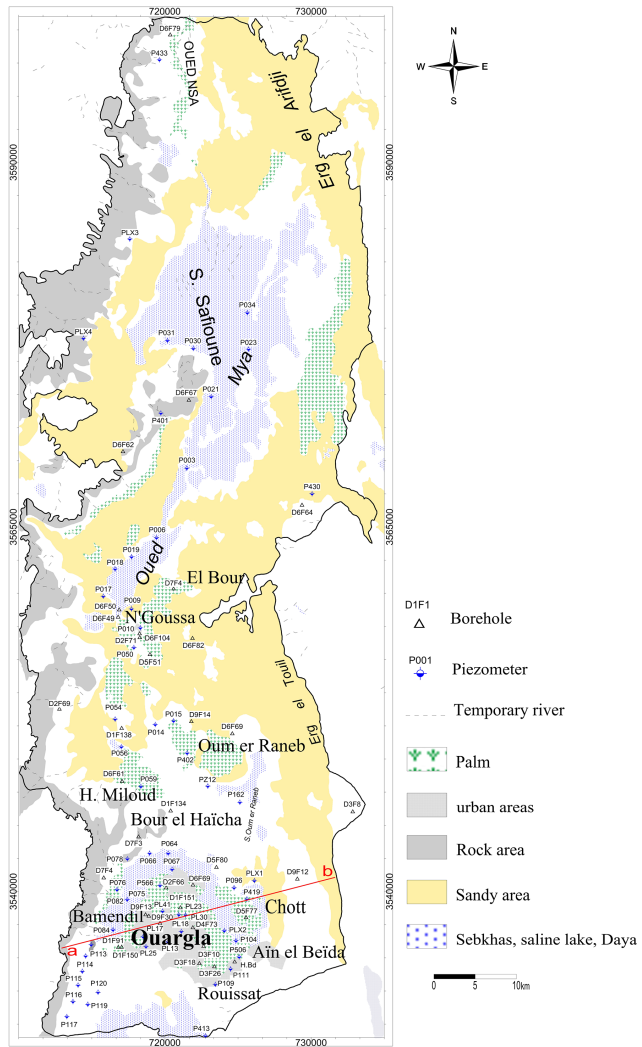


**Figure 2.** Geologic cross section in the region of Ouargla. The blue pattern used for Chott and Sebkha correspond to the limit of the saturated zone.

## Chemical and isotopic data from groundwaters in Sahara

R. Slimani et al.



- [Title Page](#)
- [Abstract](#) [Introduction](#)
- [Conclusions](#) [References](#)
- [Tables](#) [Figures](#)
- [◀](#) [▶](#)
- [◀](#) [▶](#)
- [Back](#) [Close](#)
- [Full Screen / Esc](#)
- [Printer-friendly Version](#)
- [Interactive Discussion](#)

**Figure 3.** Localisation map of sampling points.

Chemical and  
isotopic data from  
groundwaters in  
Sahara

R. Slimani et al.

<a href="#">Title Page</a>	
<a href="#">Abstract</a>	<a href="#">Introduction</a>
<a href="#">Conclusions</a>	<a href="#">References</a>
<a href="#">Tables</a>	<a href="#">Figures</a>
<a href="#">Full Screen / Esc</a>	
<a href="#">Printer-friendly Version</a>	
<a href="#">Interactive Discussion</a>	

**Chemical and isotopic data from groundwaters in Sahara**

R. Slimani et al.

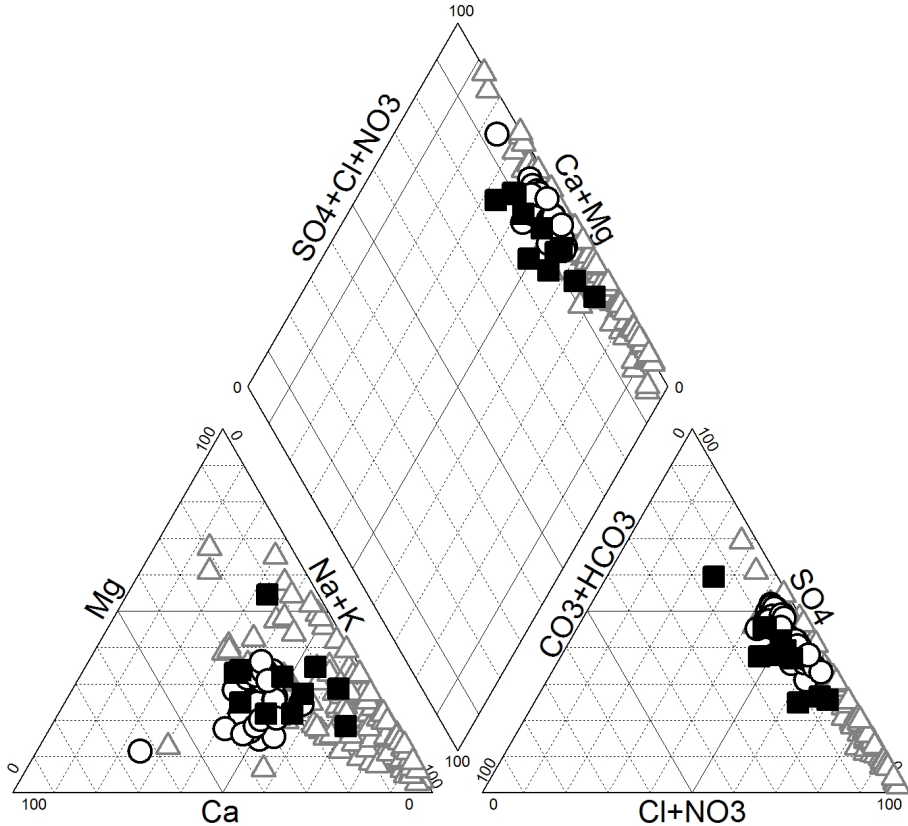


**Figure 4.** Piper diagram for Continental Intercalaire (filled squares), Complexe Terminal (open circles) and Phreatic aquifer (open triangles).

## Chemical and isotopic data from groundwaters in Sahara

R. Slimani et al.

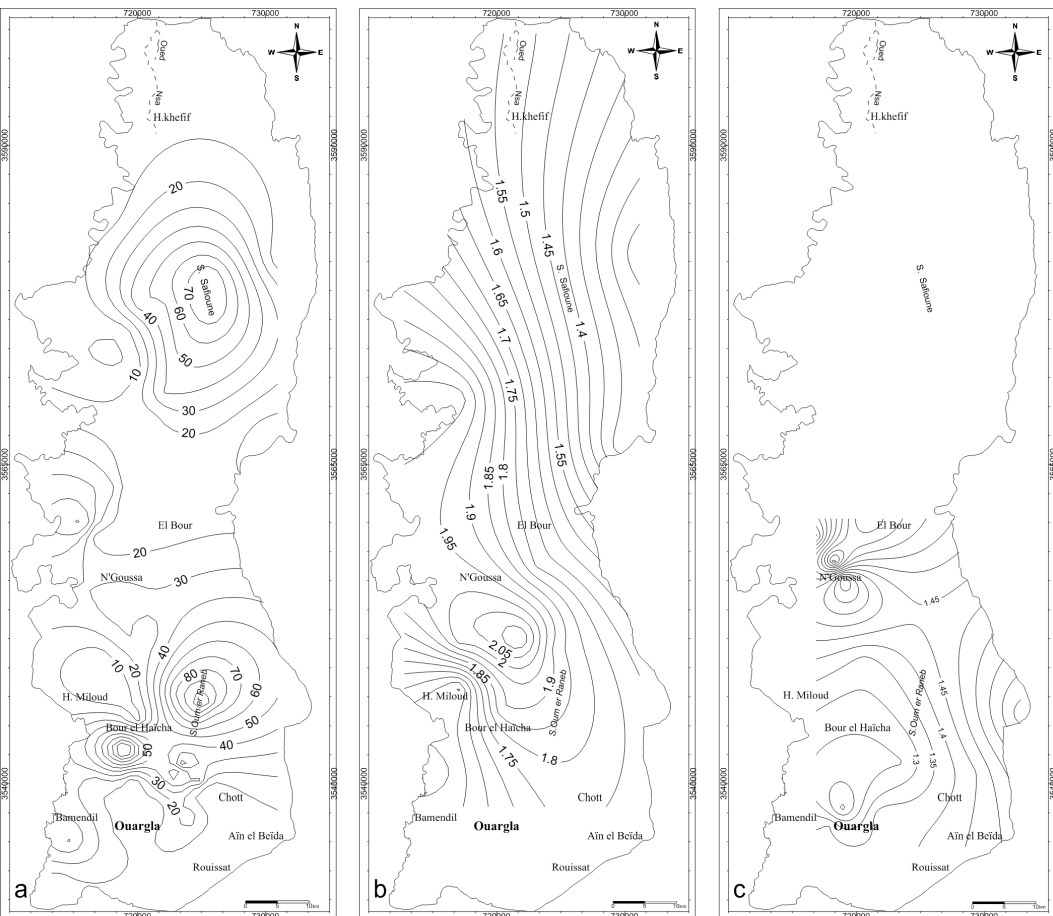


**Figure 5.** Contour maps of the salinity (expressed as global mineralization) in the aquifer system, **(a)** Phreatic aquifer; **(b)** and **(c)** Complexe Terminal [**(b)** Mio-pliocene and **(c)** Senonian]; figures are isovalues of global mineralization (values in  $\text{g L}^{-1}$ ).

## Chemical and isotopic data from groundwaters in Sahara

R. Slimani et al.

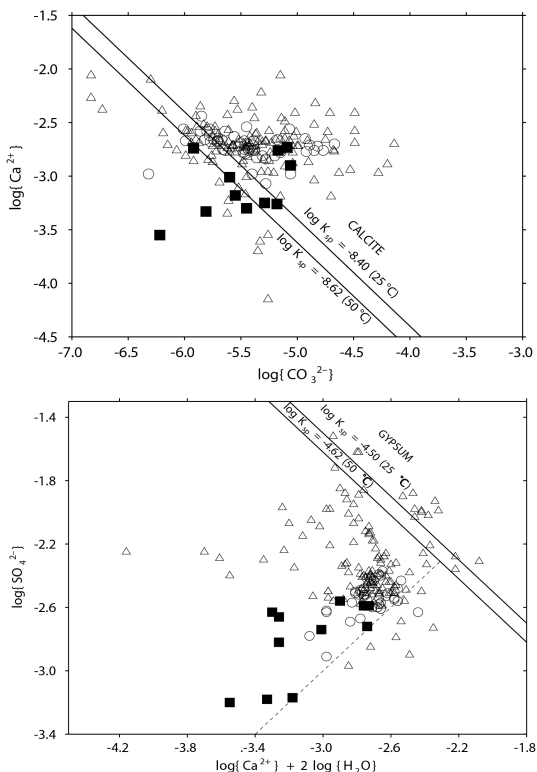


**Figure 6.** Equilibrium diagrams of calcite (top) and gypsum (bottom) for Continental Intercalaire (filled squares), Complexe Terminal (open circles) and Phreatic aquifer (open triangles). Equilibrium lines are defined as:  $\log\{\text{Ca}^{2+}\} + \log\{\text{CO}_3^{2-}\} = \log K_{\text{sp}}$  for calcite, and  $\log\{\text{Ca}^{2+}\} + 2 \log\{\text{H}_2\text{O}\} + \log\{\text{SO}_4^{2-}\} = \log K_{\text{sp}}$  for gypsum.

**Chemical and isotopic data from groundwaters in Sahara**

R. Slimani et al.

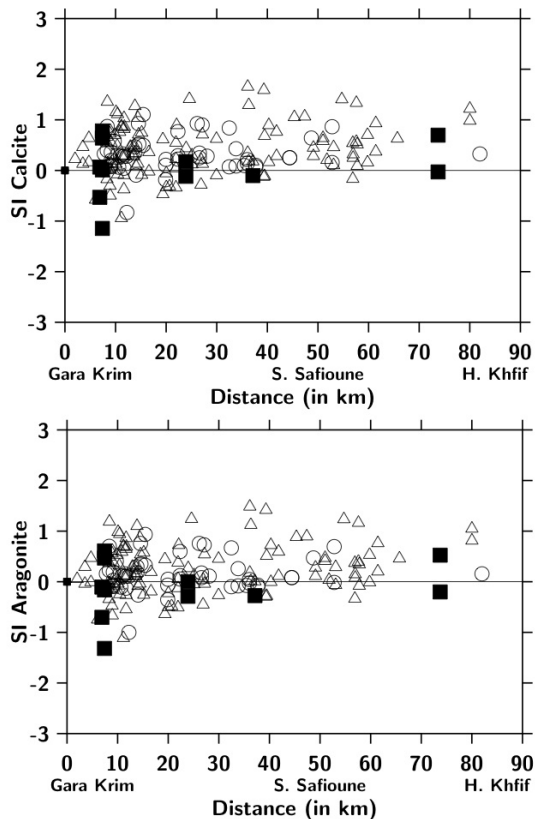


**Figure 7.** Variation of saturation indices of calcite and aragonite with distance from south to north in the region of Ouargla.

**Chemical and isotopic data from groundwaters in Sahara**

R. Slimani et al.

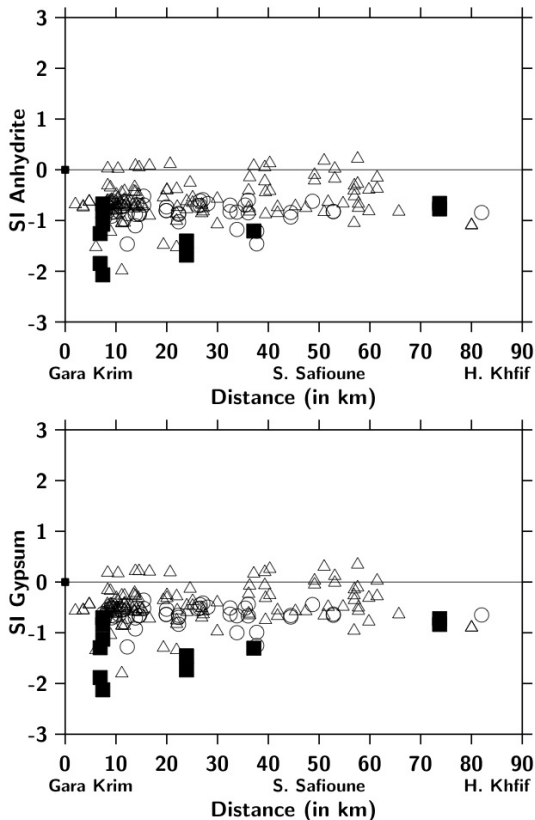


**Figure 8.** Variation of saturation indices of anhydrite and gypsum with distance from south to north in the region of Ouargla.

**Chemical and isotopic data from groundwaters in Sahara**

R. Slimani et al.

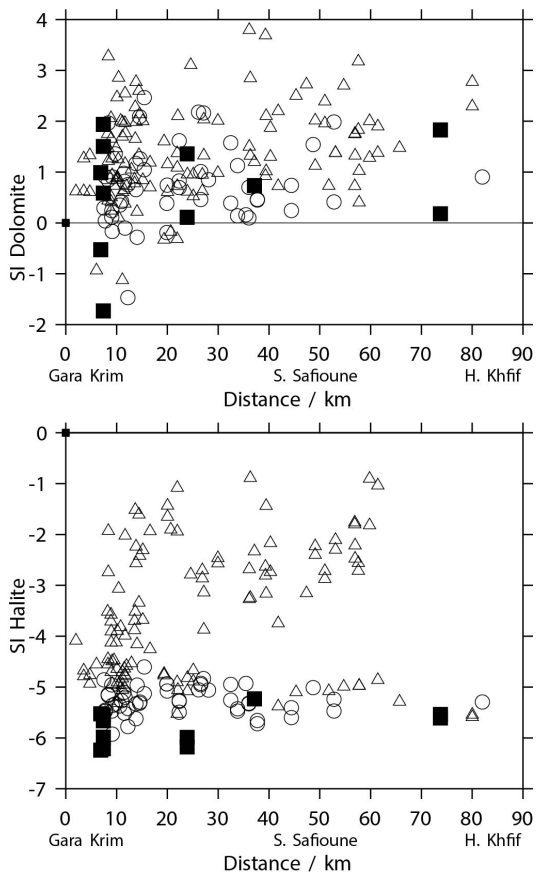


**Figure 9.** Variation of saturation indices of dolomite and halite with distance from south to north in the region of Ouargla.

Chemical and  
isotopic data from  
groundwaters in  
Sahara

R. Slimani et al.

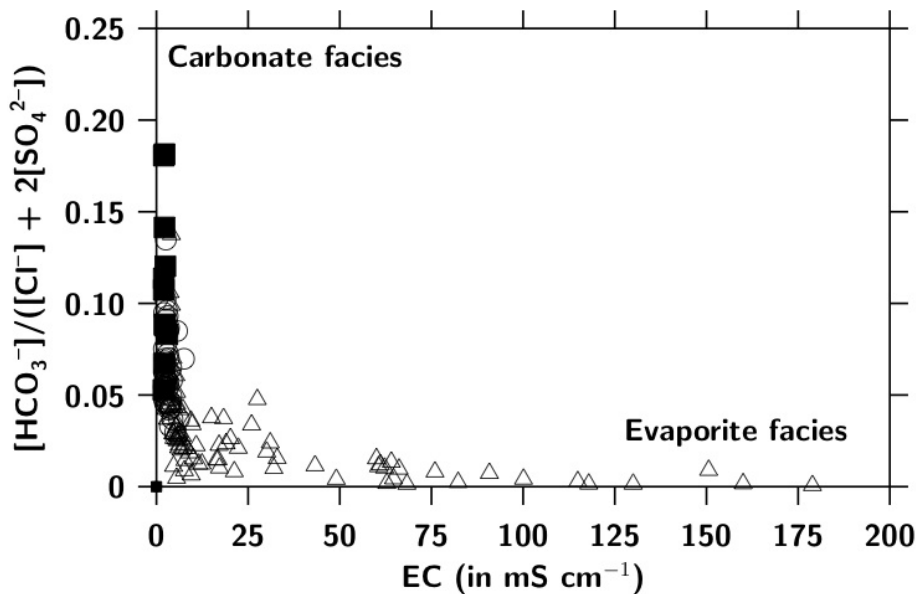


**Figure 10.** Change from carbonate facies to evaporite from Continental Intercalaire (filled squares), Complexe Terminal (open circles) and Phreatic aquifer (open triangles).

## Chemical and isotopic data from groundwaters in Sahara

R. Slimani et al.

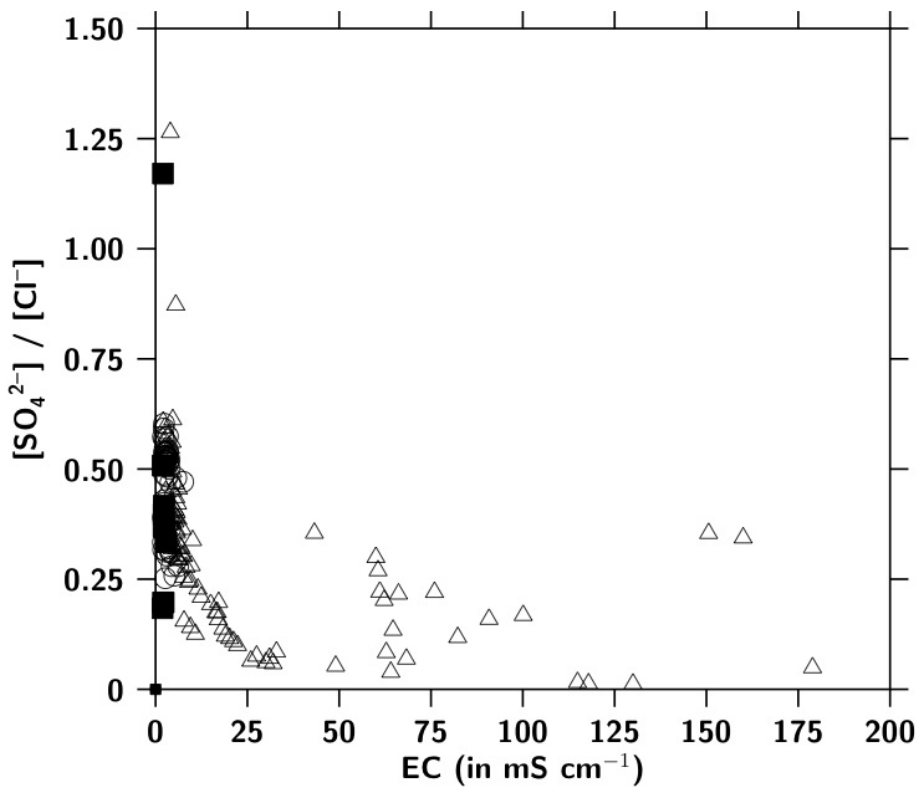


**Figure 11.** Change from sulfate facies to chloride from Continental Intercalaire (filled squares), Complexe Terminal (open circles) and Phreatic aquifer (open triangles).

**Chemical and  
isotopic data from  
groundwaters in  
Sahara**

R. Slimani et al.

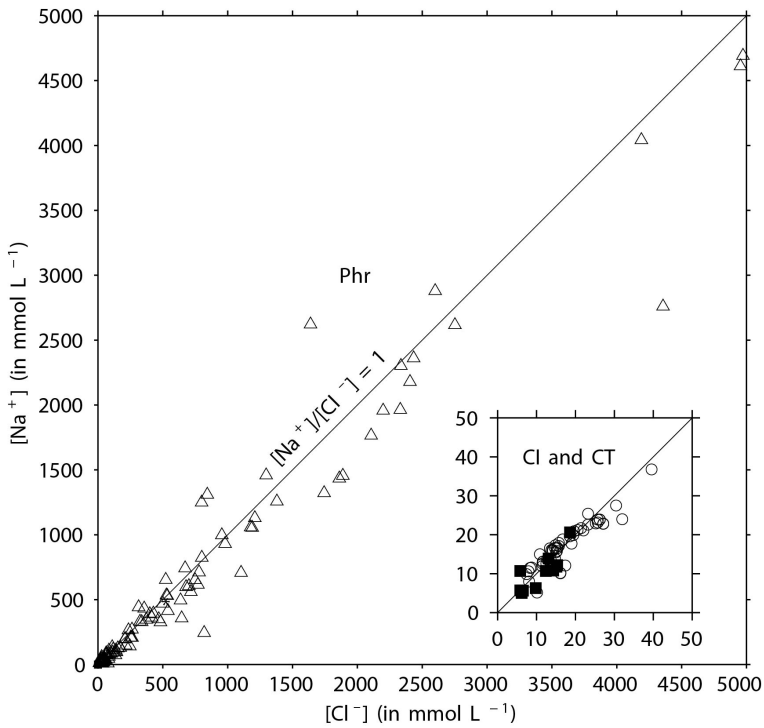


**Figure 12.** Correlation between  $\text{Na}^+$  and  $\text{Cl}^-$  concentrations in Continental Intercalaire (filled squares), Complexe Terminal (open circles) and Phreatic aquifer (open triangles). Seawater composition (star) is  $[\text{Na}^+] = 459.3 \text{ mmol L}^{-1}$  and  $[\text{Cl}^-] = 535.3 \text{ mmol L}^{-1}$  (Stumm and Morgan, 1999, p.899).

**Chemical and isotopic data from groundwaters in Sahara**

R. Slimani et al.

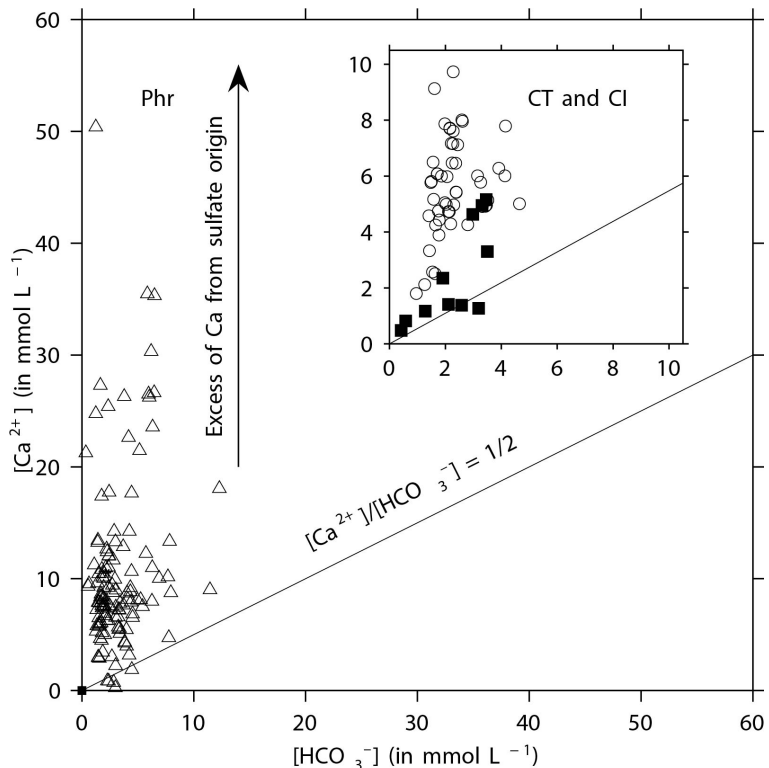


**Figure 13.** Calcium vs. HCO<sub>3</sub><sup>-</sup> diagram in Continental Intercalaire (filled squares), Complexe Terminal (open circles), Phreatic aquifer (open triangles) and Seawater composition (star) is [Ca<sup>2+</sup>] = 10.2 mmol L<sup>-1</sup> and [HCO<sub>3</sub><sup>-</sup>] = 2.38 mmol L<sup>-1</sup> (Stumm and Morgan, 1999, p.899).

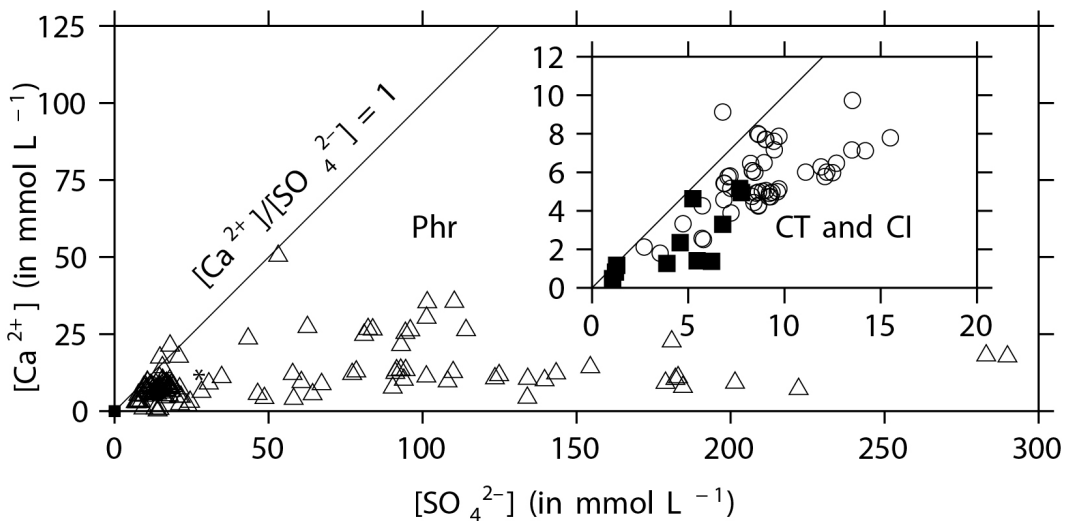


**Figure 14.** Calcium vs.  $SO_4^{2-}$  diagram in Continental Intercalaire (filled squares), Complexe Terminal (open circles), Phreatic aquifer (open triangles) and Seawater composition (star) is  $[Ca^{2+}] = 10.2 \text{ mmol L}^{-1}$  and  $[SO_4^{2-}] = 28.2 \text{ mmol L}^{-1}$  (Stumm and Morgan, 1999, p.899).

## Chemical and isotopic data from groundwaters in Sahara

R. Slimani et al.

[Title Page](#)

[Abstract](#)

[Introduction](#)

[Conclusions](#)

[References](#)

[Tables](#)

[Figures](#)

[◀](#)

[▶](#)

[◀](#)

[▶](#)

[Back](#)

[Close](#)

[Full Screen / Esc](#)

[Printer-friendly Version](#)

[Interactive Discussion](#)

**Chemical and isotopic data from groundwaters in Sahara**

R. Slimani et al.

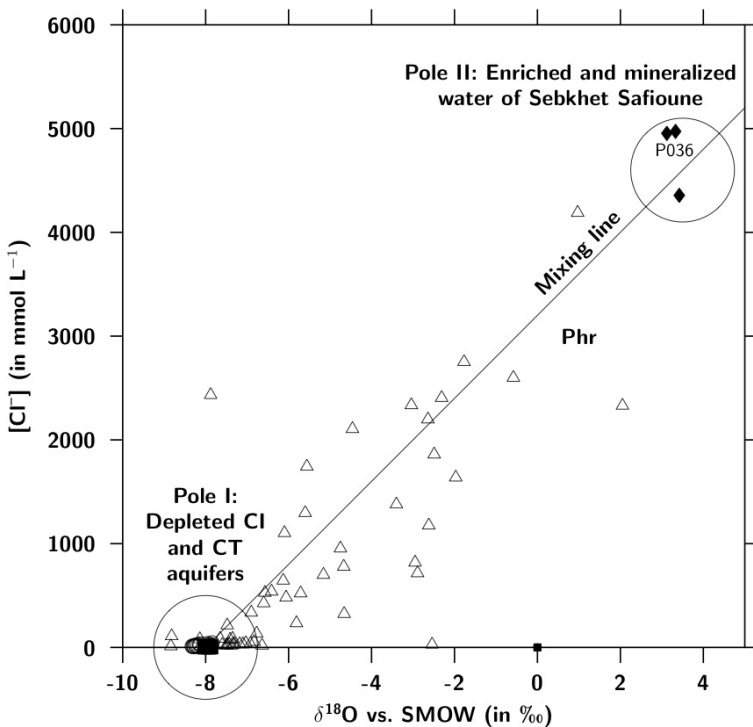


**Figure 15.** Chloride concentration vs.  $\delta^{18}\text{O}$  in Continental Intercalaire (filled squares), Complexe Terminal (open circles) and Phreatic aquifer (open triangles) from Ouargla.

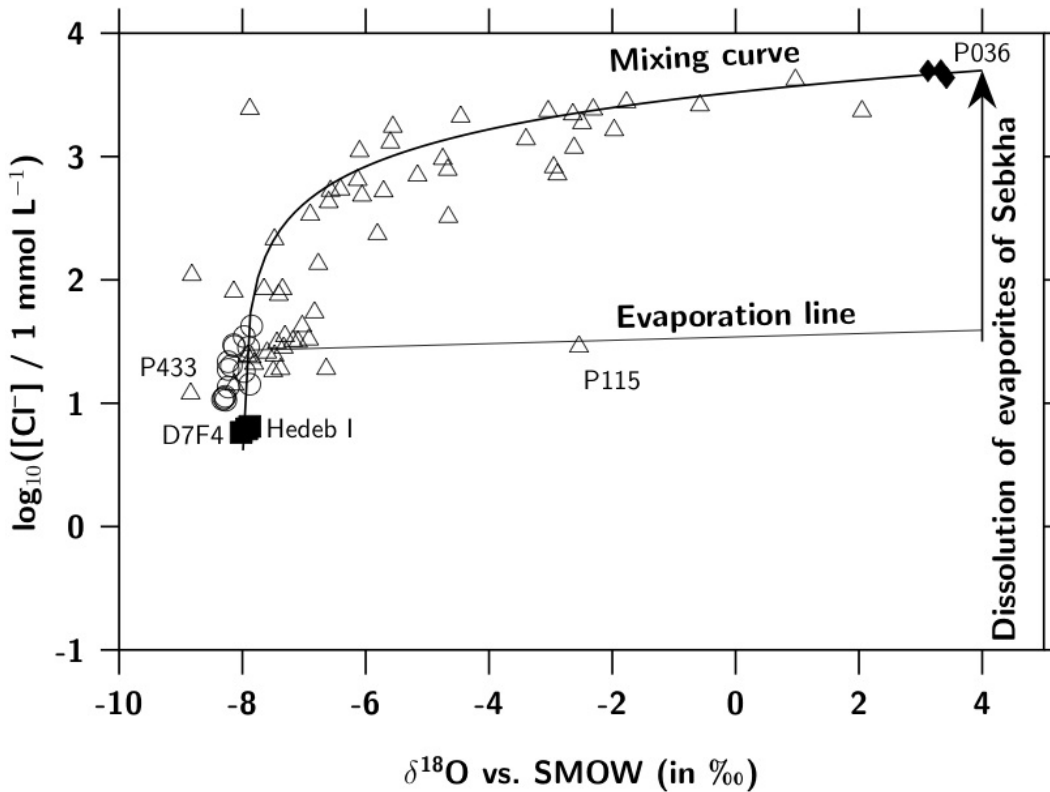


**Figure 16.** Log  $[\text{Cl}^-]$  concentration vs.  $\delta^{18}\text{O}$  in Continental Intercalaire (filled squares), Complexe Terminal (open circles) and Phreatic aquifer (open triangles) from Ouargla.

Chemical and isotopic data from groundwaters in Sahara

R. Slimani et al.

- [Title Page](#)
- [Abstract](#) [Introduction](#)
- [Conclusions](#) [References](#)
- [Tables](#) [Figures](#)
- [◀](#) [▶](#)
- [◀](#) [▶](#)
- [Back](#) [Close](#)
- [Full Screen / Esc](#)
- [Printer-friendly Version](#)
- [Interactive Discussion](#)

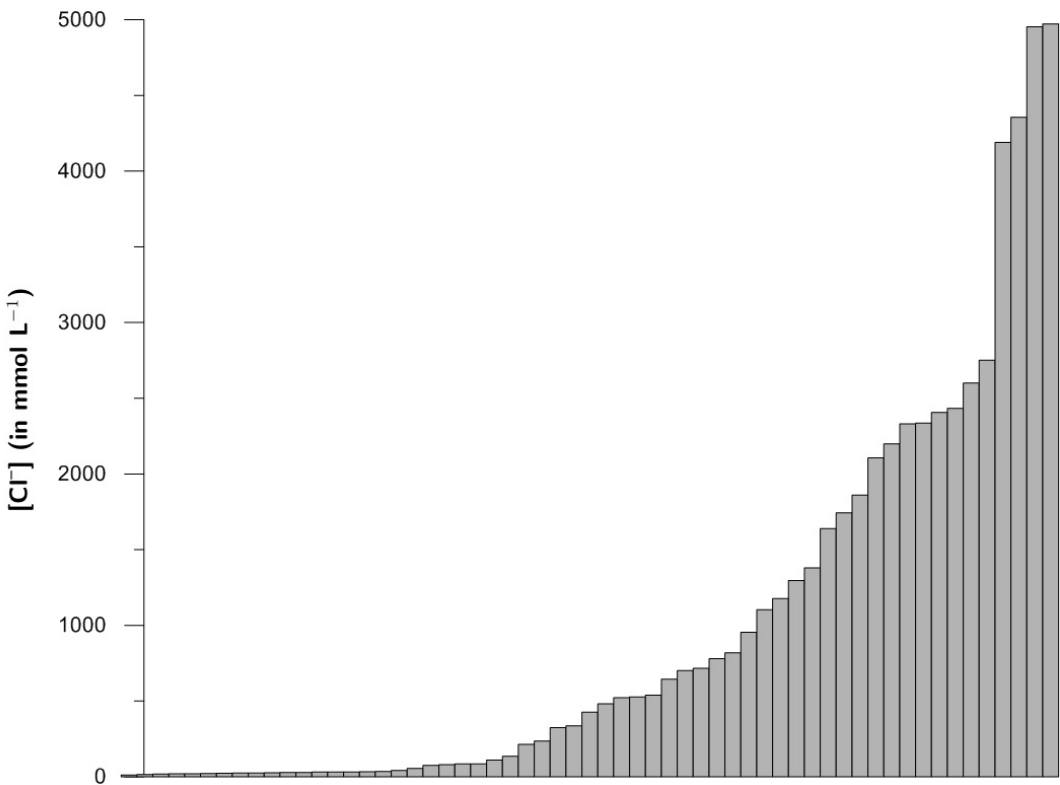


**Figure 17.** Histogram of  $\text{Cl}^-$  concentration in Phr samples from 1996 (Table 6) ( $n = 59$ ). For 17 samples,  $[\text{Cl}^-] < 35 \text{ mmol L}^{-1}$ .

## Chemical and isotopic data from groundwaters in Sahara

R. Slimani et al.

- [Title Page](#)
- [Abstract](#) [Introduction](#)
- [Conclusions](#) [References](#)
- [Tables](#) [Figures](#)
- [◀](#) [▶](#)
- [◀](#) [▶](#)
- [Back](#) [Close](#)
- [Full Screen / Esc](#)
- [Printer-friendly Version](#)
- [Interactive Discussion](#)